AMERICAN SOCIETY FOR MICROBIOLOGY | Journal of Virology®

VIRUS-CELL INTERACTIONS

Kaposi's Sarcoma-Associated Herpesvirus Immediate Early Proteins Trigger FOXQ1 Expression in Oral Epithelial Cells, Engaging in a Novel Lytic Cycle-Sustaining Positive Feedback Loop

Natalie Atyeo,[a] Min Young Chae,[a] Zsolt Toth,[a,b,c] Aria Sharma,[a] Bernadett Papp[a,b,c,d,e]

[a]Department of Oral Biology, University of Florida College of Dentistry, Gainesville, Florida, USA
[b]Genetics Institute, University of Florida, Gainesville, Florida, USA
[c]Health Cancer Center, University of Florida, Gainesville, Florida, USA
[d]Informatics Institute, University of Florida, Gainesville, Florida, USA
[e]Center for Orphaned Autoimmune Disorders, University of Florida, Gainesville, Florida, USA

ABSTRACT Kaposi's sarcoma-associated herpesvirus (KSHV) is an oncogenic gammaherpesvirus that can replicate in oral epithelial cells to promote viral transmission via saliva. To identify novel regulators of KSHV oral infection, we performed a transcriptome analysis of KSHV-infected primary human gingival epithelial (HGEP) cells, which identified the gene coding for the host transcription factor FOXQ1 as the top induced host gene. FOXQ1 is nearly undetectable in uninfected HGEP and telomerase-immortalized gingival keratinocytes (TIGK) cells but is highly expressed within hours of KSHV infection. We found that while the FOXQ1 promoter lacks activating histone acetylation marks in uninfected oral epithelial cells, these marks accumulate in the FOXQ1 promoter in infected cells, revealing a rapid epigenetic reprogramming event. To evaluate FOXQ1 function, we depleted FOXQ1 in KSHV-infected TIGK cells, which resulted in reduced accumulation of KSHV lytic proteins and viral DNA over the course of 4 days of infection, uncovering a novel lytic cycle-sustaining role of FOXQ1. A screen of KSHV lytic proteins demonstrated that the immediate early proteins ORF45 and replication and transcription activator (RTA) were both sufficient for FOXQ1 induction in oral epithelial cells, indicating active involvement of incoming and rapidly expressed factors in altering host gene expression. ORF45 is known to sustain extracellular signal-regulated kinase (ERK) p90 ribosomal s6 kinase (RSK) pathway activity to promote lytic infection. We found that an ORF45 mutant lacking RSK activation function failed to induce FOXQ1 in TIGK cells, revealing that ORF45 uses a shared mechanism to rapidly induce both host and viral genes to sustain lytic infection in oral epithelial cells.

IMPORTANCE The oral cavity is a primary site of initial contact and entry for many viruses. Viral replication in the oral epithelium promotes viral shedding in saliva, allowing interpersonal transmission, as well as spread to other cell types, where chronic infection can be established. Understanding the regulation of KSHV infection in the oral epithelium would allow for the design of universal strategies to target the first stage of viral infection, thereby halting systemic viral pathogenesis. Overall, we uncover a novel positive feedback loop in which immediate early KSHV factors drive rapid host reprogramming of oral epithelial cells to sustain the lytic cycle in the oral cavity.

KEYWORDS KSHV, ORF45, RSK, epigenetics, gene expression, herpesvirus, immediate-early protein, lytic infection, tegument

Editor Jae U. Jung, Lerner Research Institute, Cleveland Clinic

Address correspondence to Bernadett Papp, bpapp@dental.ufl.edu.

The authors declare no conflict of interest.

Received 31 October 2022
Accepted 2 February 2023
Published 23 February 2023

The oral cavity is the initial site of contact and entry for many human viruses. Viral replication in the oral epithelium allows for spread to other cell types, where chronic infection can be established (1). Additionally, viral shed in saliva promotes transmission between individuals, and the detection of high viral titers in saliva, gingival crevicular fluid, and throat wash samples underlines the clinical significance of oral viral infection (2–5).

Kaposi's sarcoma-associated herpesvirus (KSHV) is the etiologic agent of the endothelial malignancy Kaposi's sarcoma, the lymphoproliferative diseases primary effusion lymphoma and multicentric Castleman's disease, and KSHV inflammatory cytokine syndrome (KICS) (6–9). Importantly, epidemiologic studies indicate that the primary route of KSHV transmission is the oral route, via saliva. KSHV DNA has been detected in the oral cavities of infected individuals, and these individuals can exhibit recurrent viral shedding in saliva (10–14). Enhanced KSHV lytic infection in more differentiated layers of the oral epithelium provides further evidence that the oral cavity is a reservoir for infectious virus (15–17). The oral cavity is also a route of spread to other cell types, such as tonsillar B cells, which can promote KSHV spread throughout the body (18–20). Despite the biological and epidemiologic relevance of oral KSHV infection as a first step in chronic infection and pathogenesis, little is known about the key mechanisms regulating KSHV infection in the oral epithelium (reviewed in reference 21).

Similar to all herpesviruses, KSHV exhibits a biphasic lytic and latent life cycle. Upon entry into the host cell, viral recruitment of host epigenetic machinery leads to the temporally and spatially regulated heterochromatinization of the viral episome and the subsequent silencing of the KSHV lytic program (22, 23). The virus can be induced to reactivate in response to environmental stimuli such as hypoxia or secondary infections, leading to the temporally ordered expression of the full cascade of immediate early (IE), early (E), and late (L) viral genes driven by the viral replication and transcription activator (RTA), a potent activator of host and viral genes (24–27). During primary infection of most cell types *in vitro*, KSHV establishes a latent infection (28). In contrast, oral epithelial cells support productive KSHV infection, with efficient expression of KSHV lytic genes (12). Additionally, as opposed to the heterochromatin establishment on the KSHV genome that is observed in most cell types, reduced deposition of repressive chromatin marks with high levels of activating chromatin marks (e.g., histone H3 lysine 4 trimethylation [H3K4me3] and lysine 27 acetylation [H3K27ac]) were observed on the KSHV genome in infected E6/E7-immortalized oral epithelial cells (23). However, the key viral or host mechanisms that promote a permissive cellular environment supporting the KSHV lytic cycle in oral epithelial cells remain to be characterized.

In order to successfully infect host cells, KSHV hijacks host signaling pathways. During *de novo* infection, binding of KSHV envelope glycoprotein B (gB) to the host cell activates the MEK (mitogen-activated protein kinase [MAPK]/extracellular signal-regulated kinase [ERK] kinase)/ERK cascade, a MAPK pathway that is exploited by several viruses (29–31). Activation of the MEK/ERK axis during *de novo* KSHV infection and viral reactivation leads to the phosphorylation of the downstream p90 ribosomal s6 kinase (RSK) family, a group of kinases involved in regulation of cell growth, proliferation, and differentiation (32, 33). While initial KSHV infection triggers MEK/ERK/RSK activation, this activation is sustained by KSHV immediate early protein ORF45, which binds to activated ERK and RSK and prevents their dephosphorylation (34). ORF45-mediated sustained ERK/RSK activity leads to the activation of host transcriptional and translational machinery, including the c-Fos AP-1 family transcription factor and eIF4B (eukaryotic initiation factor 4B) translation initiation factor, which are critical to the viral life cycle (35–37). In addition to being classified as an immediate early gene, ORF45 is also a part of the viral tegument, which is located between the viral envelope and nucleocapsid. ORF45 is thus directly delivered into host cells during primary infection, allowing for rapid inhibition of the host antiviral interferon response (38–40). Although ORF45 plays key roles during different phases of the KSHV life cycle (reviewed in reference 41), the role of ORF45 during oral infection is still unknown.

While the modulation of host gene expression is essential for efficient KSHV infection and reactivation, much less is understood about host-pathogen interactions during the first hours of infection that might support the sustained KSHV lytic cycle in infected oral epithelial cells. To fill this knowledge gap, we performed a genome-wide gene expression analysis in KSHV-infected oral epithelial cells, which led to the subsequent identification of the rapid induction of a novel lytic cycle-sustaining host transcription factor called FOXQ1. Our study demonstrates the epigenetic reprogramming of the FOXQ1 promoter in KSHV-infected oral epithelial cells and identifies the KSHV-encoded immediate early factors RTA and ORF45 as activators of FOXQ1 gene expression, revealing a novel positive feedback loop that can support the lytic cycle in infected oral epithelial cells.

RESULTS

Primary KSHV infection of oral epithelial cells results in sustained lytic viral gene expression. While KSHV has a broad tropism, *de novo* infection of most cell types leads to the establishment of a latent infection (28). However, infectious KSHV particles have been isolated from oral samples from KSHV-infected individuals, suggesting an ability for oral epithelial cells to support lytic viral infection (12). To perform a detailed characterization of KSHV infection of oral epithelial cells *in vitro*, we infected primary human gingival epithelial (HGEP) cells as well as telomerase-immortalized gingival keratinocytes (TIGKs) with KSHV BAC16. The KSHV BAC16 clone expresses a green fluorescent protein (GFP) marker under a constitutively active host promoter, allowing for visual identification of infected cells (42). We used our previously published transgenic KSHV clone modified to carry a triple FLAG-tagged RTA gene (3×F-RTA KSHV) to aid in detection of RTA using FLAG antibody. We found a nearly 100% primary infection rate of HGEP and TIGK cells that led to sustained, gradually increasing levels of viral immediate early, early, and late genes during the 3 days following infection (HGEP data shown in Fig. 1A to C and TIGK data shown in Fig. 1D to F). A gradual increase in ORF64 late viral gene expression (Fig. 1C and F) was observed, and KSHV late protein K8.1 was detectable only after 48 hours post-infection in infected HGEP (Fig. 1B) and TIGK (Fig. 1E) cells. To block lytic viral DNA replication, KSHV-infected TIGK cells were treated with phosphonoacetic acid (PAA), an inhibitor of viral DNA synthesis, starting at 2 hpi. PAA treatment reduced viral DNA copy numbers at 72 hpi (Fig. 1G) and was accompanied by marked reduction in expression in the KSHV ORF18 and ORF33 late genes and reduced levels of late protein K8.1 (Fig. 1H and I), indicating that sustained lytic viral gene expression and DNA replication can occur during *de novo* infection of immortalized oral epithelial cells.

Characterization of host gene expression changes in primary oral epithelial cells following KSHV infection. Since KSHV encodes potent rapidly expressed viral transcription factors, we hypothesized it might be capable of reprogramming oral epithelial cells immediately after infection to promote sustained lytic infection. To identify rapidly dysregulated host genes, we characterized the global host gene expression changes in HGEP cells at 8 h following KSHV infection. To this end, total RNA was prepared from three replicates of mock-infected and KSHV-infected HGEP cells at 8 hpi. Transcriptome sequencing (RNA-seq) analysis identified 1,339 differentially expressed genes based on criteria satisfying a minimum of 2-fold differential expression and false-discovery rate (FDR) of less than 0.05 (Fig. 2A and B; Table S1). Specifically, we identified 340 host genes that were upregulated and 999 host genes that were downregulated in infected cells (Fig. 2A and B and Table S1). The group of differentially expressed genes was further analyzed to reveal enriched biological processes using Gene Ontology (GO) analysis (Tables S1 and S2). The top six biological processes identified among all of the upregulated and the downregulated genes are shown in Fig. 2C and D, while Table S2 shows the full list of identified biological process terms with associated genes in each group. The upregulated genes were enriched in key biological processes related to keratinization and cell migration (see the full list in Table S2). Interestingly, many of the upregulated genes are members of the epidermal differentiation

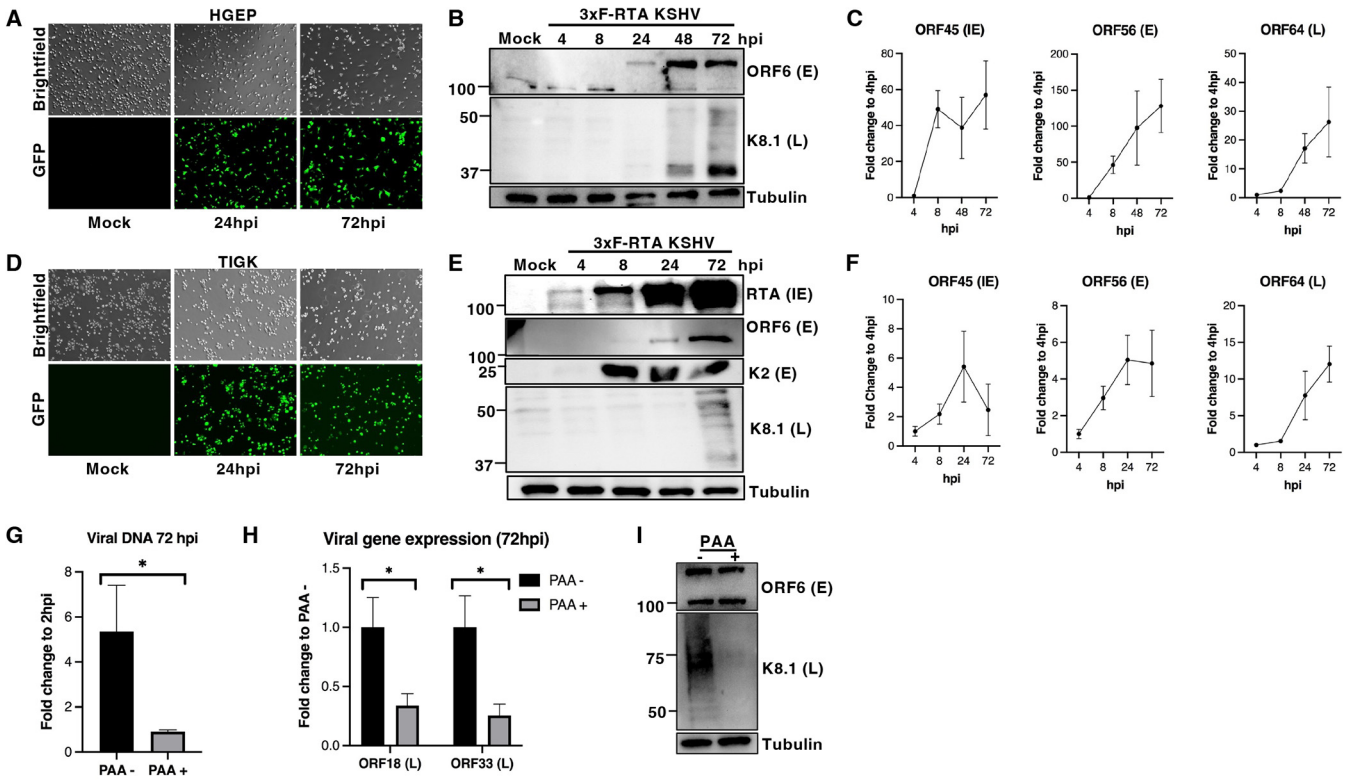

FIG 1 Sustained lytic viral gene expression during primary infection of oral epithelial cells (A) HGEP cells were infected with KSHV expressing a triple FLAG-tagged RTA gene (3×F-RTA KSHV) and collected at the indicated time points. Cells were visualized with a fluorescence microscope to identify GFP-positive (KSHV-positive) cells. (B) Immunoblot analysis of KSHV early (E) and late (L) viral proteins in KSHV-infected HGEP cells. Tubulin was used as a loading control. (C) RT-qPCR analysis of expression of representative immediate early (IE), early (E), and late (L) viral genes in KSHV-infected HGEP cells. (D) TIGK cells were infected with 3×F-RTA KSHV, and KSHV-infected cells were visualized with a fluorescence microscope. (E) Immunoblot analysis of IE, E, and L viral proteins in KSHV-infected TIGK cells. FLAG antibody was used to detect 3×FLAG-tagged RTA. (F) RT-qPCR analysis of representative IE, E, and L viral genes in KSHV-infected TIGK cells. (G) TIGK cells were infected with wild-type KSHV BAC16 and treated with 100 μM PAA, starting at 2 hpi, for 72 h. Viral DNA was purified, and viral copy number was measured by qPCR and compared to that in the nontreated (PAA−) infected cells. (H) RT-qPCR analysis of KSHV late gene expression upon PAA treatment at 72 hpi; (I) immunoblot analysis of KSHV early and late genes in PAA-treated cells versus control (PAA−) cells. *, $P < 0.05$.

complex (EDC) genes (e.g., genes coding for late cornified envelope proteins 3D and 3E [LCE3D and LCE3E]). Among the most induced genes, we also identified genes coding for transcription factors involved in regulation of development, such as PRDM1, FOXQ1, and FOXF2 (Fig. 2C and Table S1 and S2). We also found that several of the induced genes encode proteins that are negative regulators of cell proliferation (Fig. 2C and Table S1 and S2). In accordance with this, regulation of DNA replication initiation was found to be the most enriched biological process in the group of downregulated genes, a group of genes that includes cell cycle regulators such as cyclins and DNA replication factors (Fig. 2D and Table S1 and S2). Altogether, these findings highlight a rapid alteration of the host transcriptome related to cell cycle regulation in oral epithelial cells during KSHV infection whose significance in oral KSHV infection needs to be evaluated in future studies. Importantly, our results are consistent with another transcriptome study, which found that several differentiation-related genes, such as the EDC genes (e.g., the LCE3D gene) and genes encoding master regulatory factors (e.g., PRDM1), were among the induced host genes in human immortalized oral keratinocytes (HOK16B) exposed to KSHV-derived virus-like vesicles (VLVs), which lack viral genomes (43). Furthermore, our findings are also consistent with a recent state-of-the-art single-cell RNA-seq study describing dysregulated EDC genes in KSHV-infected oral epithelial 3D cultures (16).

Notably, we identified the FOXQ1 gene and the related FOXF2 gene among the top induced human genes in HGEP cells upon KSHV infection (Fig. 2B). Importantly, FOXQ1 is a critical regulator of cellular differentiation (44–49), and FOXQ1 is known to be

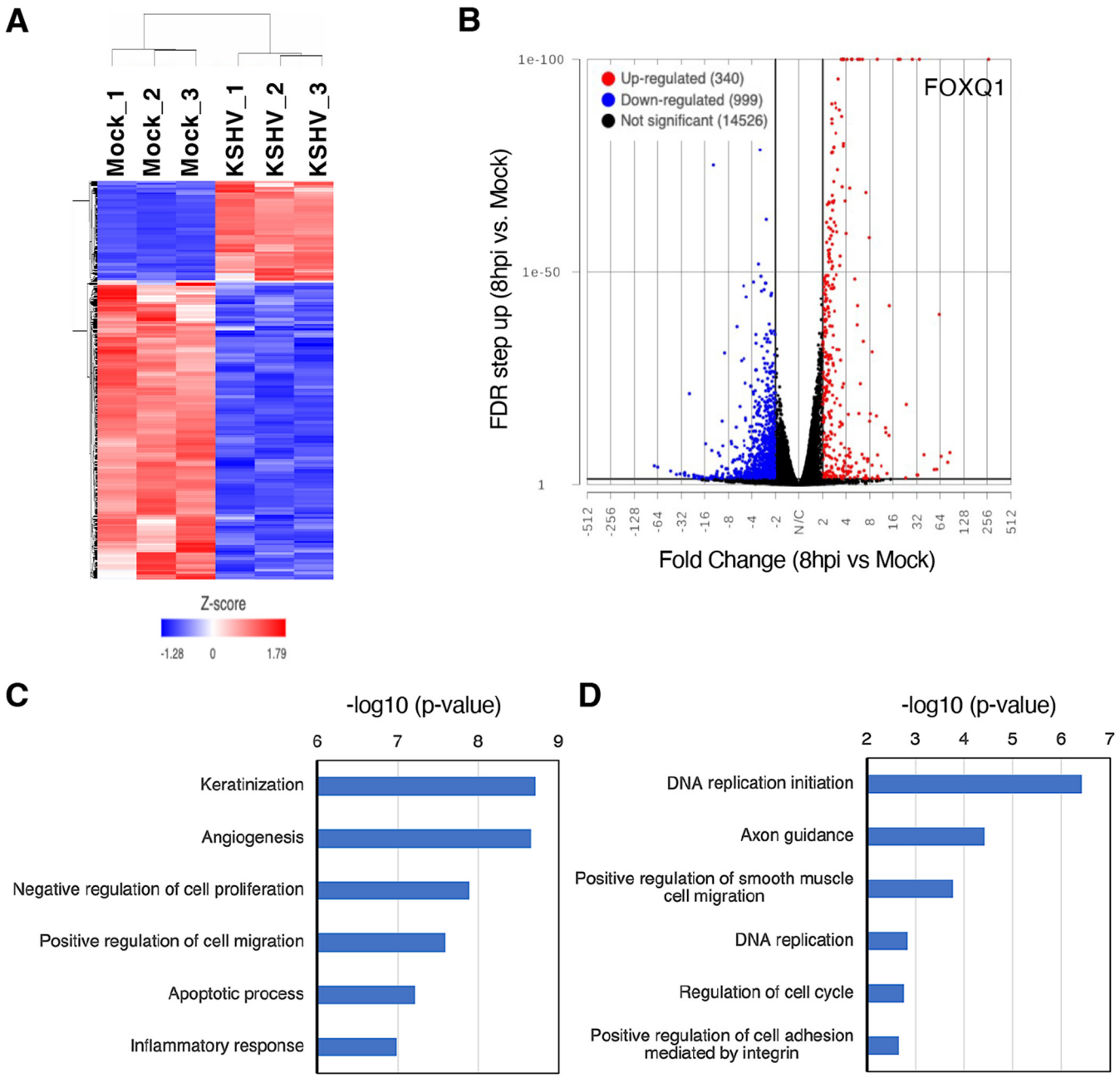

FIG 2 Characterization of host gene expression changes in primary oral epithelial cells following KSHV infection. (A) Hierarchical clustering of 1339 differentially expressed host genes in primary oral epithelial cells following KSHV infection at 8 hpi compared to mock-infected cells, including the genes expressed at least 2-fold differentially, with an FDR cutoff of <0.05 and Z-score values indicated below. (B) Volcano plot depicting host genes, with the *x* axis showing fold change between KSHV-infected and mock-infected HGEP cells and the *y* axis depicting the corresponding FDR values. Genes at least 2-fold differentially expressed, with an FDR cutoff of <0.05, were examined to identify up- and downregulated genes. The 340 upregulated host genes in infected cells are colored in red. FOXQ1 and FOXF2 genes are indicated. The 999 downregulated host genes in infected cells are colored in blue. (C and D) Gene Ontology analysis of the 340 upregulated genes (C) and the 999 downregulated genes (D), with a graph depicting the top identified biological processes as a highlight of the full Gene Ontology result, which is provided in the supplemental material.

induced under skin differentiation-promoting conditions (50). However, the function of FOXQ1 in viral infections is still unknown. To confirm the findings of our RNA-seq analysis in HGEP cells and to determine the stage-specific kinetics of FOXQ1 gene expression following KSHV infection, we collected mock- and KSHV-infected HGEP and TIGK cells at several time points. We found that while FOXQ1 levels remained almost undetectable in uninfected HGEP and TIGK cells, FOXQ1 was rapidly induced upon KSHV infection by 4 hpi and peaked at 8 hpi, followed by a gradual decline in both HGEP

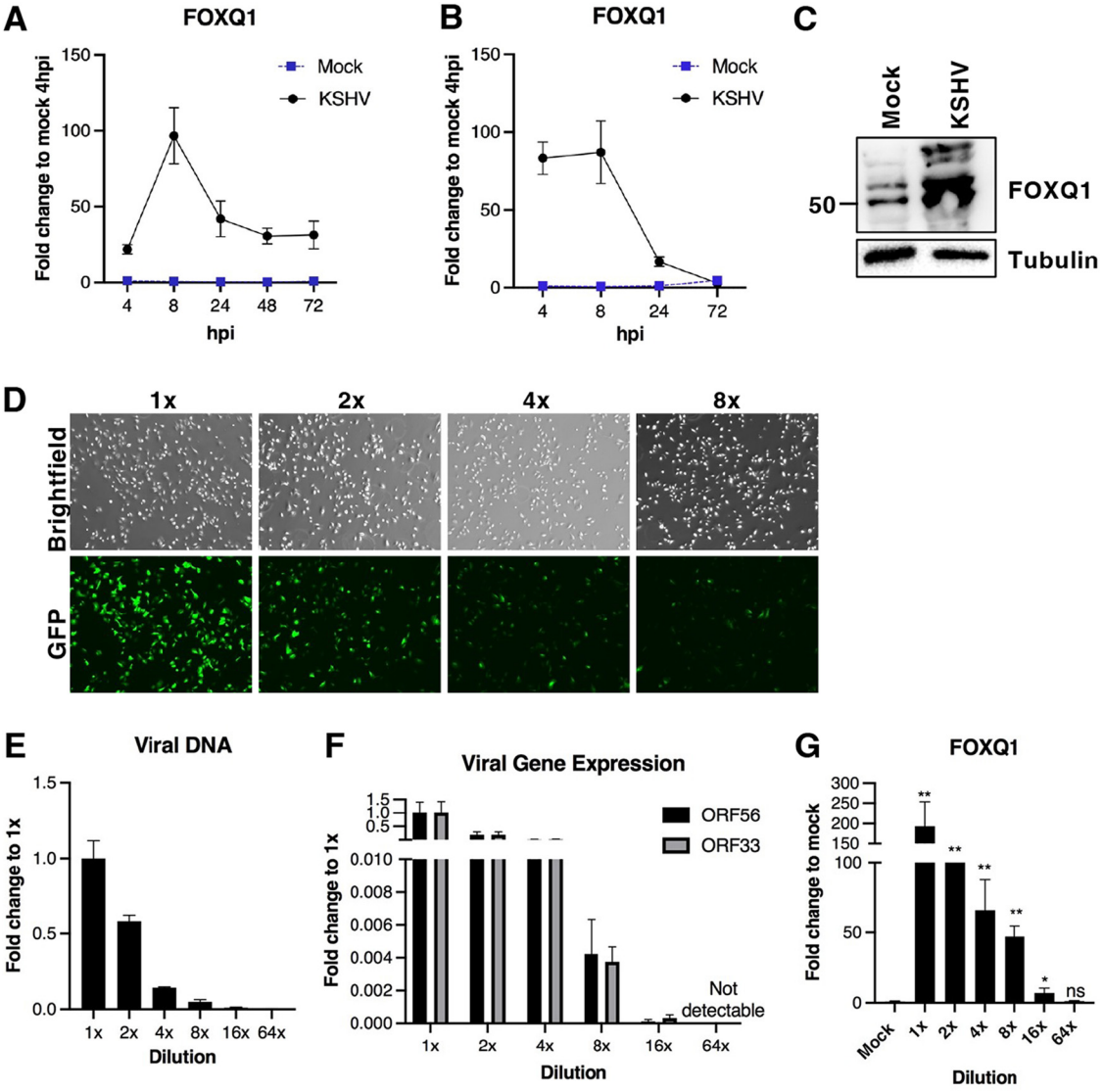

FIG 3 FOXQ1 expression kinetics in KSHV-infected oral epithelial cells (A and B) RT-qPCR analyses of FOXQ1 expression in mock-infected or KSHV-infected cells at the indicated time points in (A) HGEP cells and (B) TIGK cells. (C) Immunoblot analysis of FOXQ1 protein in mock-infected or KSHV-infected TIGK cells at 24 hpi. (D) HGEP cells were infected with 2-fold serial dilutions of KSHV BAC16 virus stock (where 1× refers to our standard KSHV titer, with a nearly 100% infection rate in oral epithelial cells), and fluorescence microscopy was used to visualize KSHV-infected (GFP-positive) HGEP cells at 24 hpi. (E) qPCR analysis of intracellular viral DNA; (F) RT-qPCR analysis of representative early (ORF56) and late (ORF33) viral genes at the indicated viral titers. (G) RT-qPCR analysis of FOXQ1 levels at the corresponding viral titers calculated as a fold change from uninfected cells. *, $P < 0.05$; **, $P < 0.01$; ns, not significant.

(Fig. 3A) and TIGK (Fig. 3B) cells. In accordance with the increased FOXQ1 transcript level, we observed greater abundance of FOXQ1 protein at 1 day postinfection in TIGK cells (Fig. 3C). As FOXQ1 has relevant biological functions in cellular differentiation, and the gene encoding it was also the most robustly induced host gene during KSHV infection in oral epithelial cells, we primarily focused on FOXQ1 in our following analyses.

FOXQ1 expression positively correlates with viral titer and viral gene expression in HGEP cells. To further establish the link between FOXQ1 expression levels and KSHV infection, we infected HGEP cells with decreasing amount of KSHV virus and analyzed viral and FOXQ1 gene expression at 24 hpi. As anticipated, infection of HGEP cells with smaller amounts of KSHV led to a commensurate decrease in GFP-positive cells (Fig. 3D), viral DNA copy (Fig. 3E), and early (ORF56) and late (ORF33) viral gene expression (Fig. 3F). Notably, the FOXQ1 transcript level was more than 200-fold higher in HGEP cells following infection with our standard KSHV infection condition (1×) than

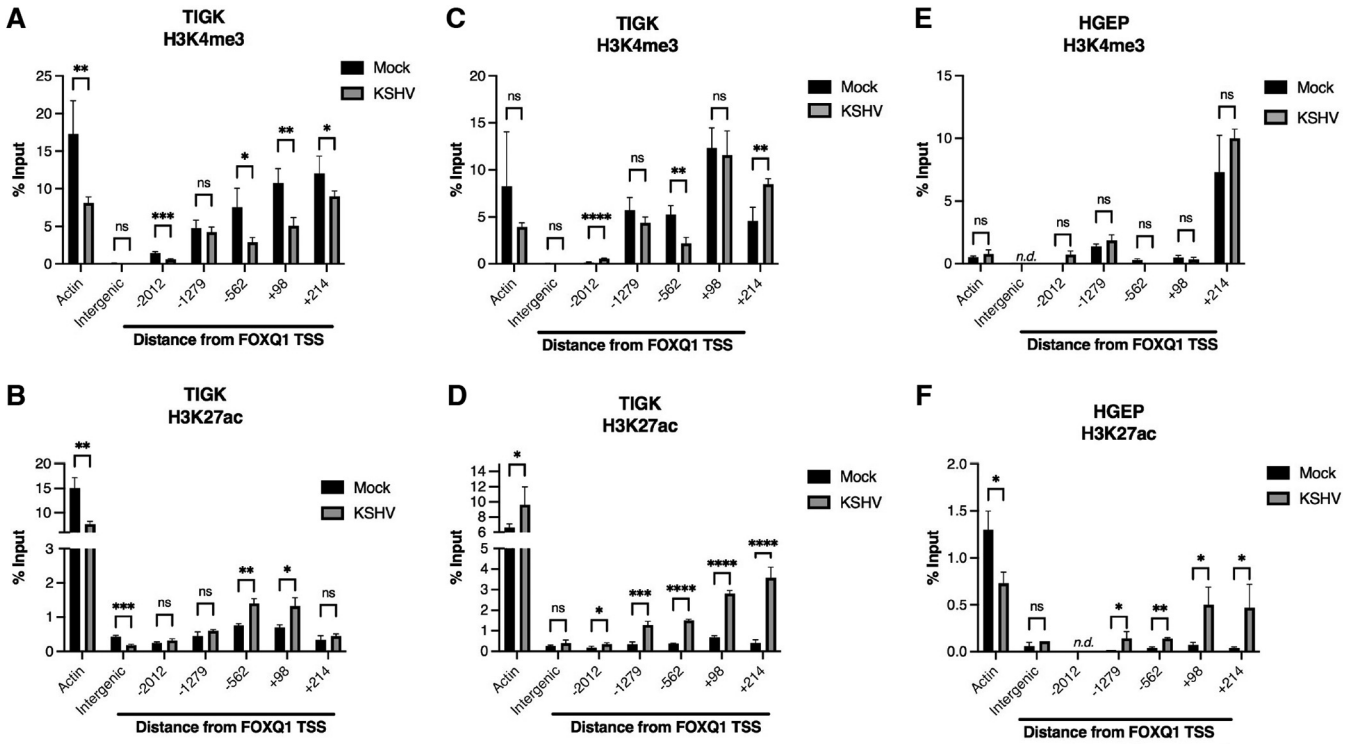

FIG 4 KSHV infection triggers accumulation of activating H3K27ac marks on the FOXQ1 promoter Chromatin immunoprecipitation (ChIP) was performed with anti-H3K4me3 antibody at 4 hpi (A) and 24 hpi (C) and anti-H3K27ac antibody at 4 hpi (B) and 24 hpi (D) in mock- and KSHV-infected TIGK cells. ChIP was performed in HGEP cells at 24 hpi with anti-H3K4me3 antibody (E) and anti-H3K27ac (F). qPCR was used to quantify histone mark enrichment at the indicated distances from the FOXQ1 transcription start site (TSS). The actin gene is a constitutively expressed host gene, while the intergenic region is a region without gene expression. Enrichment of each histone mark was calculated as a percentage of the total chromatin input. *, $P < 0.05$; **, $P < 0.01$; ***, $P < 0.001$; ****, $P < 0.0001$; ns, not significant.

that in mock-infected HGEP cells, and a gradual decrease in FOXQ1 level was observed with a lower KSHV infection rate (Fig. 3G). FOXQ1 was still clearly induced even at the 8× dilution condition, when there was a very low KSHV infection rate as shown by GFP positivity. FOXQ1 was not significantly induced compared to mock-infected cells at the point at which viral gene expression became undetectable, suggesting a tight link between high KSHV infection level and a high FOXQ1 expression level in oral epithelial cells.

FOXQ1 promoter accumulates activating acetylation marks in KSHV-infected oral epithelial cells. Given the rapid induction of FOXQ1, we hypothesized that a preexisting permissive epigenetic landscape on its regulatory region might allow for rapid induction following KSHV infection. To characterize the chromatin state of the FOXQ1 regulatory region, we performed chromatin immunoprecipitation followed by quantitative real-time PCR analysis (ChIP-qPCR) in mock-infected and KSHV-infected oral epithelial cells at 4 hpi (Fig. 4A and B) and 24 hpi (Fig. 4C to F) and tested for the presence of activating H3K4me3 and H3K27ac histone marks in the proximal promoter region of the FOXQ1 gene. Since key gene regulatory elements are often found in close proximity to the transcription start sites (TSSs) of genes, we focused on the region directly 2 kb upstream of the FOXQ1 TSS and 0.2 kb immediately downstream in the beginning of the FOXQ1 gene body. We found that several areas of the tested FOXQ1 regulatory region were already enriched in activating H3K4me3 marks in uninfected cells and remained enriched in KSHV-infected TIGK cells at 4 hpi (Fig. 4A) and 24 hpi (Fig. 4C) and in HGEP cells at 24 hpi (Fig. 4E). KSHV infection led to a slight decrease in H3K4me3 in the regions tested. Additionally, while the entire region surrounding the FOXQ1 TSS lacked detectable activating H3K27ac marks in uninfected HGEP and TIGK cells compared to the negative-control intergenic region, H3K27ac marks began to accumulate specifically at the TSS area in KSHV-infected TIGK cells as early as 4 hpi (Fig. 4B). The entire FOXQ1 promoter region displayed

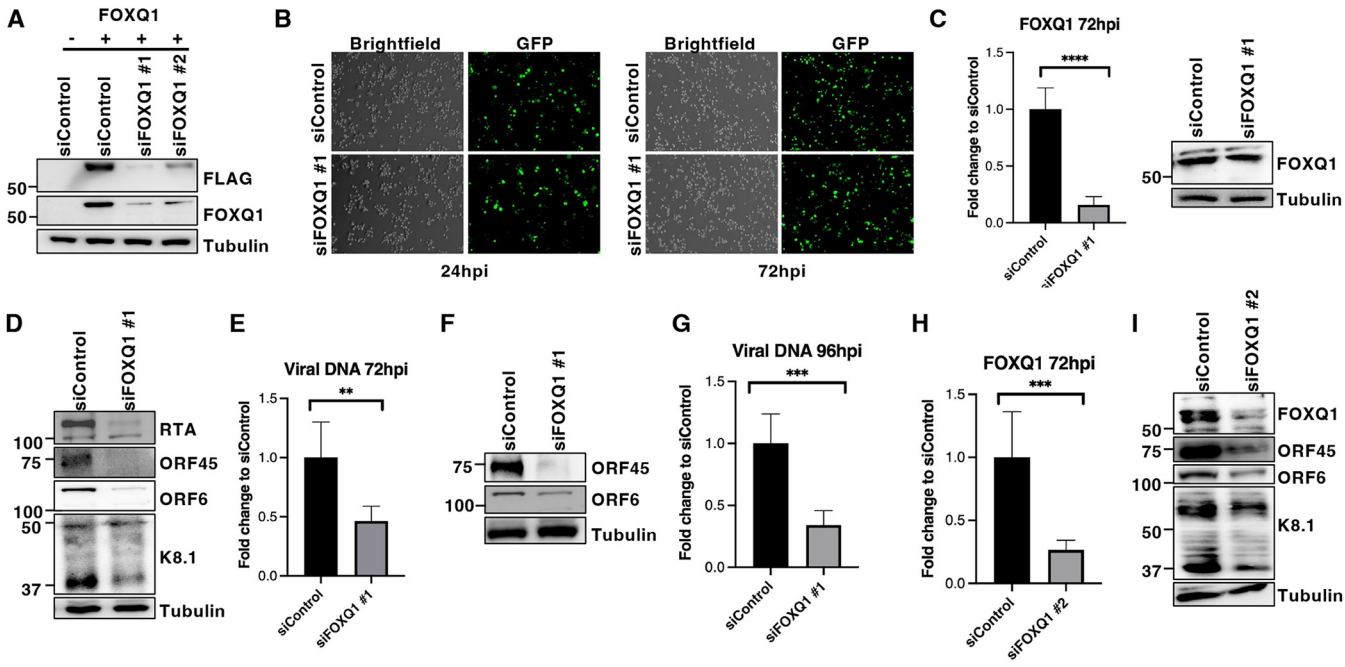

FIG 5 FOXQ1 sustains the KSHV lytic cycle in oral epithelial cells (A) FLAG-tagged FOXQ1 or empty vector was transfected in 293T cells for 24 h, and then cells were treated with control siRNAs targeting a nonmammalian luciferase gene (referred to as siControl) or two independent FOXQ1 siRNAs (siFOXQ1 1 or 2), and FOXQ1 levels were analyzed by immunoblotting with FLAG and FOXQ1 antibodies. (B) TIGK cells were infected with KSHV and treated with siControl or siFOXQ1 1 at 2 hpi. KSHV-infected cells (GFP positive) were visualized using fluorescence microscopy at 24 and 72 hpi. (C) RT-qPCR and immunoblot analysis of FOXQ1 levels in siRNA-treated, KSHV-infected TIGK cells at 72 hpi; (D and E) immunoblot analysis of viral protein levels (D) and qPCR analysis of combined intracellular and extracellular viral DNA levels (E) at 72 hpi. (F and G) Immunoblot analysis of viral protein levels (F) and qPCR analysis of viral DNA levels (G) at 96 hpi. (H and I) TIGK cells were infected with KSHV and then treated with an independent siRNA (siFOXQ1 2) at 2 hpi and collected at 72 hpi. (H and I) RT-qPCR analysis of FOXQ1 expression (H) and immunoblot of viral proteins (I) at 72 hpi. **, $P < 0.01$; ***, $P < 0.001$; ****, $P < 0.0001$.

high H3K27ac enrichment at 24 hpi in both cell types, with some regions exhibiting levels close to the constitutively expressed actin gene promoter (Fig. 4D and F). These results demonstrate that while the FOXQ1 promoter is enriched with the H3K4me3 euchromatin mark, it is largely devoid of the H3K27ac chromatin opening mark in uninfected oral epithelial cells, in accordance with its almost undetectable expression. Importantly, we showed that KSHV infection triggers a rapid epigenetic reprogramming of the entire FOXQ1 promoter region in oral epithelial cells into classical hallmarks of highly active promoter/proximal enhancer regions, with a dually enriched activating H3K4me3 and hyperacetylated H3K27ac euchromatin signature.

FOXQ1 is required for sustaining lytic KSHV infection in oral epithelial cells. Though specific Forkhead factors are known to regulate viral infections in a context-specific manner (51–54), the function of FOXQ1 in viral infections remains unknown. The rapid epigenetic reprogramming and robust induction of FOXQ1 upon KSHV infection of oral epithelial cells prompted us to investigate the potential role of FOXQ1 in the viral lytic cycle. We used two independent pools of small interfering RNAs (siRNAs) targeting FOXQ1, which we confirmed to efficiently deplete FOXQ1 protein expression in HEK293T kidney epithelial cells transfected with FLAG-FOXQ1 plasmid (Fig. 5A). We treated TIGK cells with siFOXQ1 1 starting at 2 h after KSHV infection, which did not affect the KSHV-infected oral epithelial cells morphologically and resulted in similar numbers of GFP-positive cells at 24 and 72 hpi (Fig. 5B). FOXQ1 mRNA levels were reduced by siFOXQ1 1 at 72 hpi (Fig. 5C). Strikingly, FOXQ1 depletion resulted in decreased KSHV immediate early (RTA and ORF45), early (ORF6), and late (K8.1) protein levels at 72 hpi (Fig. 5D) as well as viral DNA level at 72 hpi (Fig. 5E). A similar reduction in viral gene expression (Fig. 5F) and viral DNA copy (Fig. 5G) was observed at 96 hpi. In addition, depletion of FOXQ1 with an independent siRNA (siFOXQ1 2) also led to similarly reduced lytic viral protein levels at 72 hpi (Fig. 5H and I) These results indicate that FOXQ1 contributes to sustaining high levels of KSHV lytic proteins in oral epithelial cells.

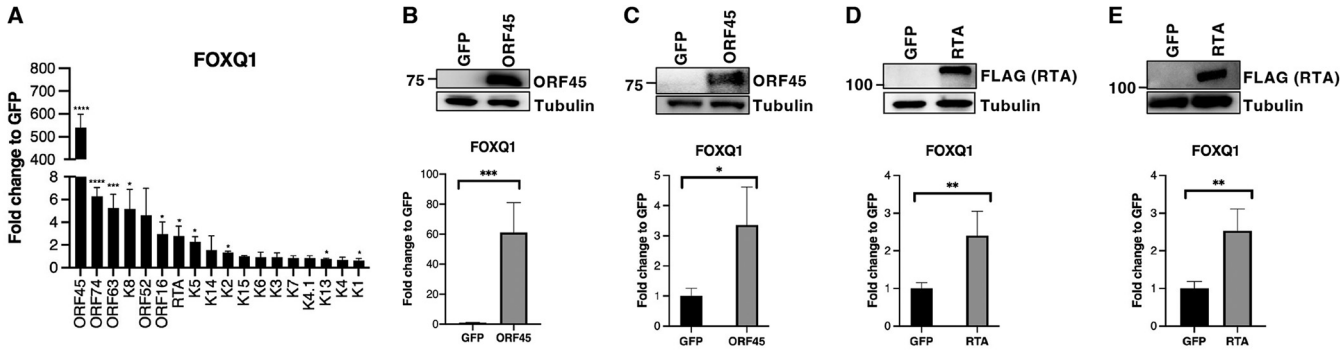

FIG 6 Screen identifies viral factors regulating FOXQ1 in oral epithelial cells. (A) HGEP cells were transduced with a lentiviral library of 18 KSHV lytic factors or GFP control lentivirus, and mRNA levels of FOXQ1 were measured at 48 h postransduction. (B) TIGK cells were transduced with GFP lentivirus or an ORF45-expressing lentivirus and collected at 48 hpi. Results from immunoblot analysis of ORF45 levels and RT-qPCR analysis of FOXQ1 are shown (C) TIGK cells were transfected with GFP or ORF45 and collected at 30 hpi. ORF45 protein levels are shown by immunoblotting, and FOXQ1 levels are shown by RT-qPCR. (D and E) HGEP cells (D) and TIGK cells (E) were transduced with either a lentivirus expressing GFP or 3×FLAG-tagged RTA. Results from immunoblot analysis of RTA expression levels and RT-qPCR analysis of FOXQ1 expression levels are shown. *, $P < 0.05$; **, $P < 0.01$; ***, $P < 0.001$; ****, $P < 0.0001$.

Identification of viral factors regulating FOXQ1 expression. We predicted that incoming and/or immediate early (IE) or early (E) viral factors might be activators of the KSHV-induced host gene coding for FOXQ1, given its rapid induction in oral epithelial cells upon KSHV infection. To test this hypothesis, we set out to identify lytic viral factors which are sufficient to induce FOXQ1 in primary human oral epithelial cells. To this end, we performed a lentiviral screen with a library of 18 KSHV factors that are involved in regulation of immune response, signaling pathways, and gene transcription and measured the expression of FOXQ1 (Fig. 6A). We identified several lytic viral factors, including the immediate early proteins ORF45 and replication and transcription activator (RTA), that were able to induce FOXQ1 (Fig. 6A).

Notably, all tested KSHV tegument proteins (ORF45, ORF52, and ORF63) induced FOXQ1 expression to some extent (Fig. 6A). ORF45, ORF52, and ORF63 all exert functions that allow viral evasion of the host immune response (38, 55, 56), but their roles in oral viral infection are largely unknown. Importantly, ORF45 was the strongest inducer of FOXQ1 in HGEP cells. We confirmed that both lentiviral expression of ORF45 (Fig. 6B) and ORF45 expression plasmid transfection (Fig. 6C) induced FOXQ1 expression in TIGK cells.

We were also particularly interested in the novel role of RTA as a FOXQ1 inducer as the host gene activation role of RTA is consistent with its well-established transcription activator function, and we and others have previously demonstrated the role of RTA in inducing key host genes during lytic reactivation (25, 57, 58). We repeated the experimental condition used for the screen to confirm the novel role of RTA as a FOXQ1 inducer both in HGEP cells (Fig. 6D) and in TIGK cells (Fig. 6E). Since both ORF45 and RTA are immediate early proteins, and ORF45 is also a tegument protein, ORF45 and RTA would be present shortly after primary infection and able to rapidly trigger FOXQ1 expression in oral epithelial cells.

RTA is not essential for FOXQ1 induction during KSHV infection of oral epithelial cells. As RTA was among the viral factors capable of inducing FOXQ1 expression in HGEP and TIGK cells and also drives expression of KSHV lytic genes, we wanted to determine if RTA is essential for FOXQ1 induction in the context of KSHV infection. In order to analyze the requirement for RTA in FOXQ1 induction, we used 3×FLAG-tagged RTA knockout (3×F-RTAKO) KSHV as well as the control 3×FLAG-tagged RTA-expressing (3×F-RTA) KSHV for infection (59). TIGK cells were infected with equal titers of 3×F-RTA KSHV and 3×F-RTAKO KSHV, as demonstrated by comparable viral DNA copies at 2 hpi (Fig. 7A). As expected, primary infection with 3×F-RTAKO KSHV led to defective lytic gene expression in TIGK cells compared to 3×F-RTA KSHV (Fig. 7B and C) as RTA is essential to induce KSHV lytic cycle. However, FOXQ1 was induced at similar levels upon infection with either the 3×FLAG-RTA or the RTAKO KSHV at 24 hpi (Fig. 7D) suggesting that

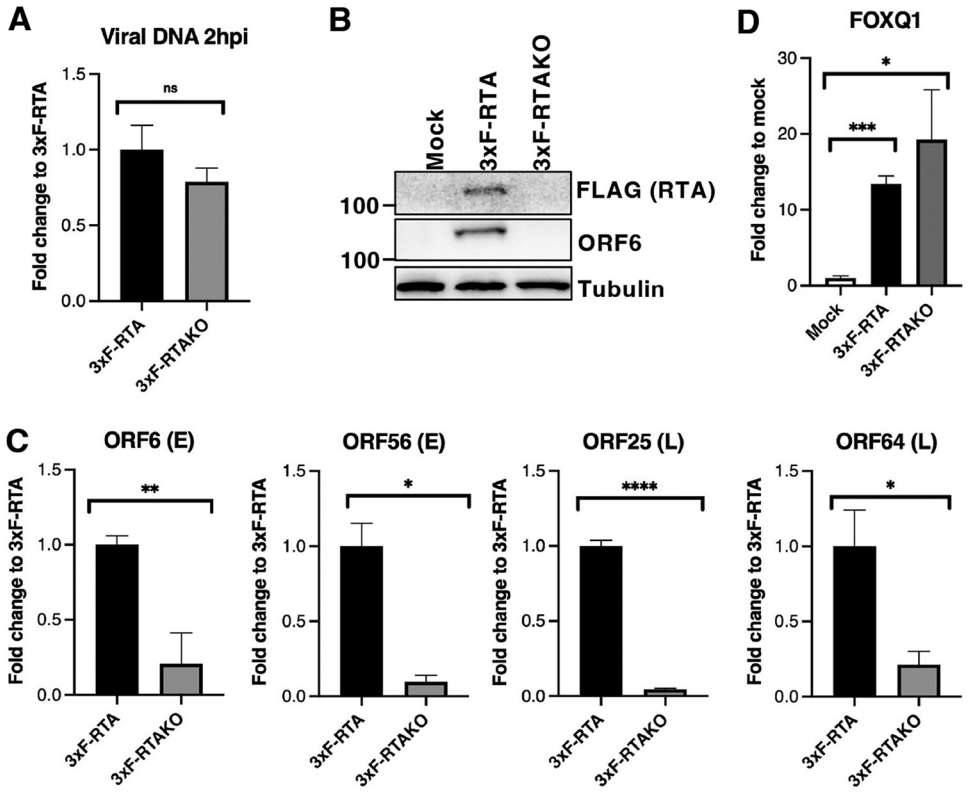

FIG 7 RTA is not essential for FOXQ1 induction following KSHV infection. TIGK cells were infected with either 3×F-RTA or 3×F-RTAKO KSHV or mock infected. (A) qPCR analysis of intracellular viral DNA at 2 hpi; (B and C) immunoblot analysis of viral proteins (B) and RT-qPCR analysis of viral gene expression (C) at 24 hpi; (D) RT-qPCR analysis of FOXQ1 expression at 24 hpi. *, $P < 0.05$; **, $P < 0.01$; ***, $P < 0.001$; ****, $P < 0.0001$.

RTA is not essential for the induction of FOXQ1 in KSHV-infected oral epithelial cells. Furthermore, since RTA drives the expression of lytic viral genes, our result demonstrates that RTA-dependent downstream viral gene expression is not required for FOXQ1 induction and provides additional evidence for the role of virion-associated tegument proteins in FOXQ1 induction.

FOXQ1 induction by KSHV lytic factors is cell-type specific. Next, we tested whether FOXQ1 induction by KSHV infection is unique to oral epithelial cells or is cell type independent. First, we infected 293T cells with KSHV (Fig. 8A) which resulted in the expression of the latent (LANA) gene, and detectable expression of the lytic (ORF56) gene (Fig. 8B). The detection of lytic genes following infection of 293T cells is in line with previous studies showing limited amount of lytic gene expression in this cell type (60). We found that in contrast to primary infection of oral epithelial cells, KSHV infection of 293T cells did not lead to an induction of FOXQ1 at 4 hpi or 24 hpi (Fig. 8C). Since ORF45 was the strongest inducer of FOXQ1 among the tested lytic factors in oral epithelial cells, we expressed ORF45 in 293T cells and 293TBAC16 cells, which harbor a latent KSHV genome. Unlike in oral epithelial cells, lentivirus-mediated ORF45 expression was unable to induce FOXQ1 expression in 293T cells (Fig. 8D) or in 293TBAC16 cells (Fig. 8E), revealing cell type specificity of ORF45-mediated FOXQ1 induction. Since ORF45 is highly expressed during lytic reactivation, we also reactivated 293TBAC16 cells with sodium butyrate (NaB), a histone deacetylase (HDAC) inhibitor, which led to increased viral gene expression, as expected (Fig. 8F), and a clear but moderate increase in FOXQ1 levels (Fig. 8G). Since HDAC inhibition can lead to accumulation of acetylation marks and chromatin opening, we also tested the effect of NaB treatment alone on the KSHV-free 293T cell line. Indeed, a similar increase in FOXQ1 levels was seen in KSHV-free 293T cells (Fig. 8H), revealing that histone deacetylase

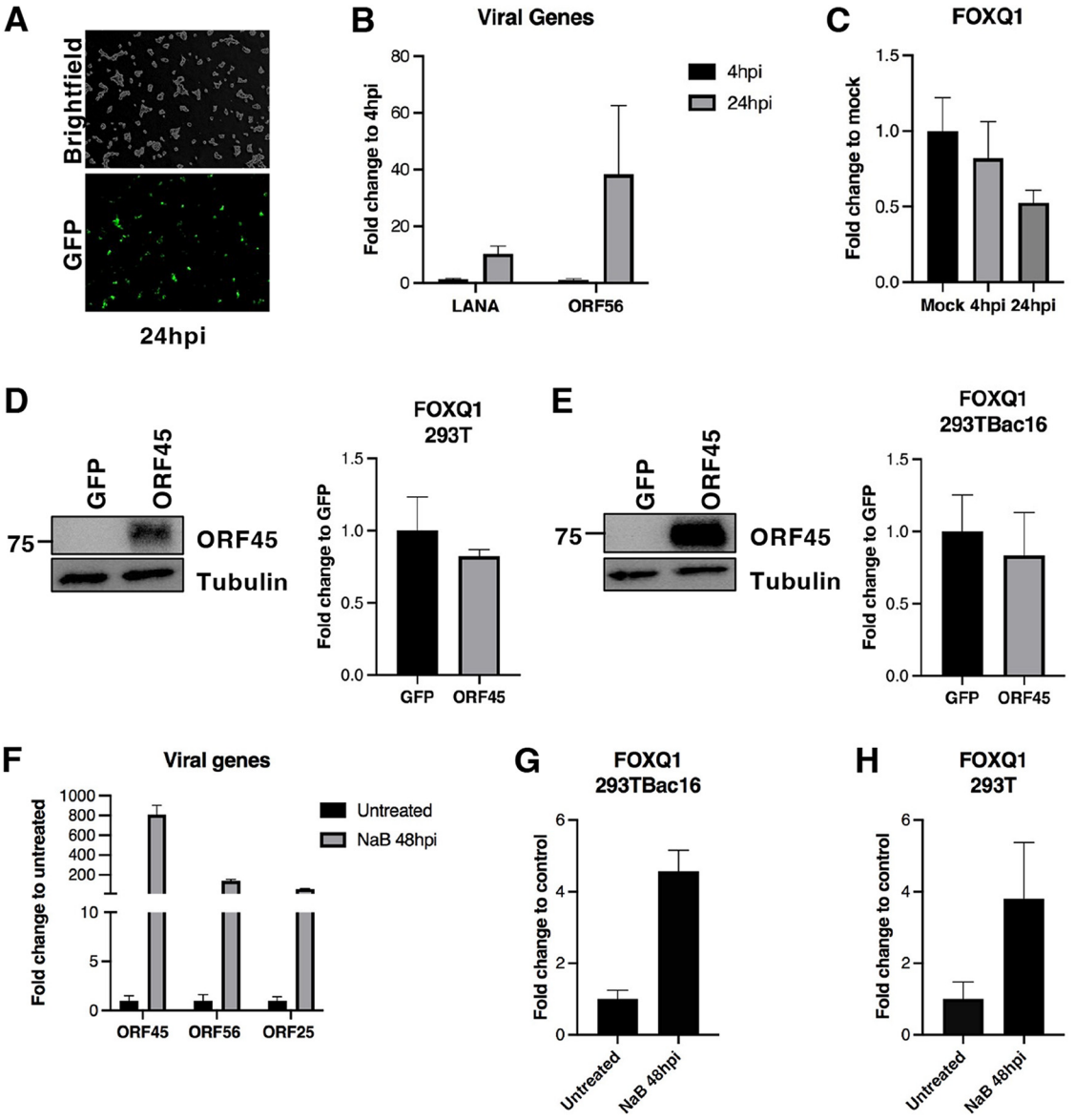

FIG 8 FOXQ1 induction by KSHV lytic factors is cell type specific. (A to C) 293T cells were infected with KSHV and collected at 4 and 24 hpi. (A) Infected cells were visualized at 24 hpi using fluorescence microscopy. (B) RT-qPCR analysis of latent (LANA) and lytic (ORF56) KSHV gene expression at 4 hpi and 24 hpi. (C) RT-qPCR analysis of FOXQ1 levels calculated as a fold change from mock-infected cells. (D and E) 293T cells (D) or 293TBAC16 cells (E) were transduced with GFP or ORF45 lentivirus and collected at 48 hpi. ORF45 protein levels are shown by immunoblotting, and FOXQ1 levels were measured by RT-qPCR. (F) 293TBAC16 cells were treated with 3 mM sodium butyrate (NaB) for 2 days to induce reactivation. (F and G) Expression of viral genes (F) and FOXQ1 levels (G) as measured by RT-qPCR. (H) 293T cells were treated with 3 mM sodium butyrate for 2 days, and FOXQ1 levels were measured by RT-qPCR.

inhibition likely directly led to increased FOXQ1 gene expression. These results support the notion that the induction of FOXQ1 by ORF45 is cell type specific. We envision that the chromatin of FOXQ1 is largely cell type specific and highly regulated by unique epigenetic mechanisms, which can affect the ability of ORF45 to induce FOXQ1 expression.

ORF45-mediated sustained activation of the ERK/RSK pathway is necessary for FOXQ1 induction. Since ORF45 is a tegument protein and we demonstrated that ORF45 was the strongest inducer of FOXQ1 in oral epithelial cells (Fig. 6A), we predicted that ORF45 itself might be the essential trigger for FOXQ1 induction in KSHV-infected oral epithelial cells and RTA could be dispensable due to its redundancy with the incoming ORF45 protein. A well-characterized role of ORF45 is the sustained activation of the downstream MEK/ERK signaling mediator, the p90 ribosomal s6 kinase (RSK), through prevention of ERK and RSK dephosphorylation (32, 34). Following KSHV

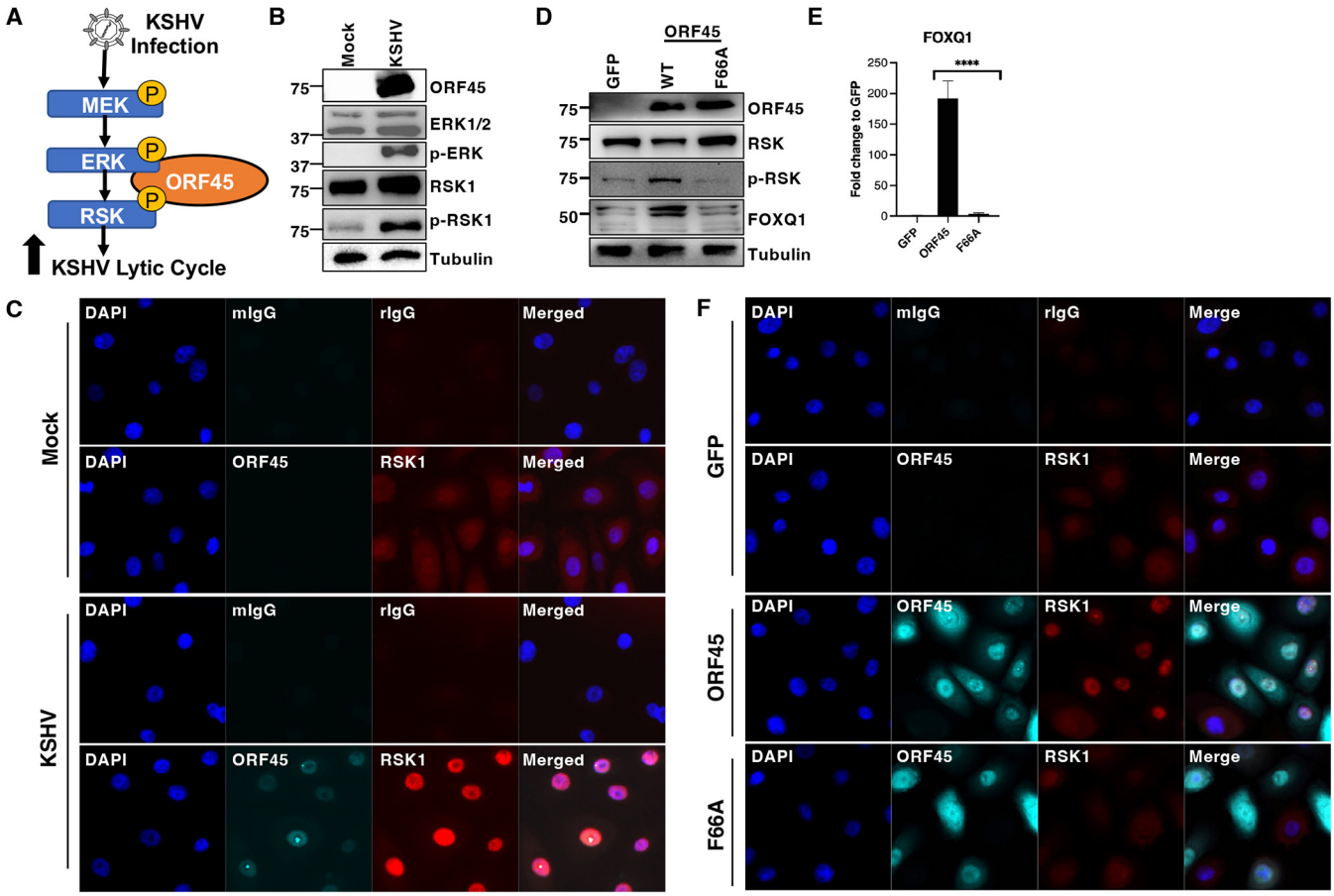

FIG 9 ORF45-mediated sustained activation of the ERK/RSK pathway is necessary for FOXQ1 induction (A) Schematic demonstrating the known mechanism of ORF45-sustained activation of the MEK/ERK/RSK cascade during KSHV infection (B) TIGK cells were infected with KSHV, and viral protein levels and markers of ERK pathway activation (p-ERK and p-RSK) were analyzed by immunoblotting at 8 hpi. (C) Immunofluorescence analysis of mock- versus KSHV-infected TIGK cells at 4 hpi. ORF45 (teal) and RSK1 (red) were detected with ORF45 and RSK1 antibodies, and anti-mouse/anti-rabbit IgGs were used as a control. DAPI was used to visualize nuclei (blue). (D to F) TIGK cells were transduced with GFP, ORF45, or ORF45-F66A mutant lentiviruses and collected at 24 h postransduction. (D) Immunoblot analysis of ORF45 and ERK/RSK markers. (E) Immunoblotting (left) and RT-qPCR analysis (right) of FOXQ1 levels; (F) immunofluorescence analysis of lentivirus-transduced TIGK cells. The same immunofluorescence staining conditions and magnification were used as in panel C.

primary infection or reactivation, ORF45-mediated sustained ERK/RSK signaling promotes viral lytic gene expression and virion production (32, 61) (Fig. 9A) First, we tested whether KSHV infection of oral epithelial cells also engages the ERK/RSK pathway, as has been shown in other cell types. We observed high expression of ORF45 as well as elevated levels of phosphorylated ERK and RSK in KSHV-infected TIGK cells at 8 hpi, which indicates that KSHV infection also sustains activation of the ERK/RSK pathway in oral epithelial cells (Fig. 9B). Immunofluorescence analysis of KSHV-infected TIGK cells revealed that ORF45 protein is mainly nuclear at 4 hpi and that KSHV infection results in nuclear accumulation of RSK1, which strongly colocalized with ORF45 in the nucleus (Fig. 9C).

To determine whether ORF45-driven FOXQ1 induction was dependent on RSK activation, we cloned an ORF45 mutant with a point mutation (F66A) abolishing its ERK/RSK binding and activation (62). Elevated p-ERK was observed in both the wild-type ORF45 and the F66A mutant lentivirus-transduced TIGK cells, but only the wild-type ORF45 was able to trigger an elevated p-RSK level (Fig. 9D). Moreover, while ORF45 induced FOXQ1 expression in TIGK cells, the F66A mutation abrogated the ability of ORF45 to induce FOXQ1 (Fig. 9E). While both wild-type and F66A mutant ORF45 accumulated in both the nucleus and the cytoplasm of TIGK cells, only wild-type ORF45 and not the F66A mutant triggered RSK1 nuclear accumulation in TIGK cells

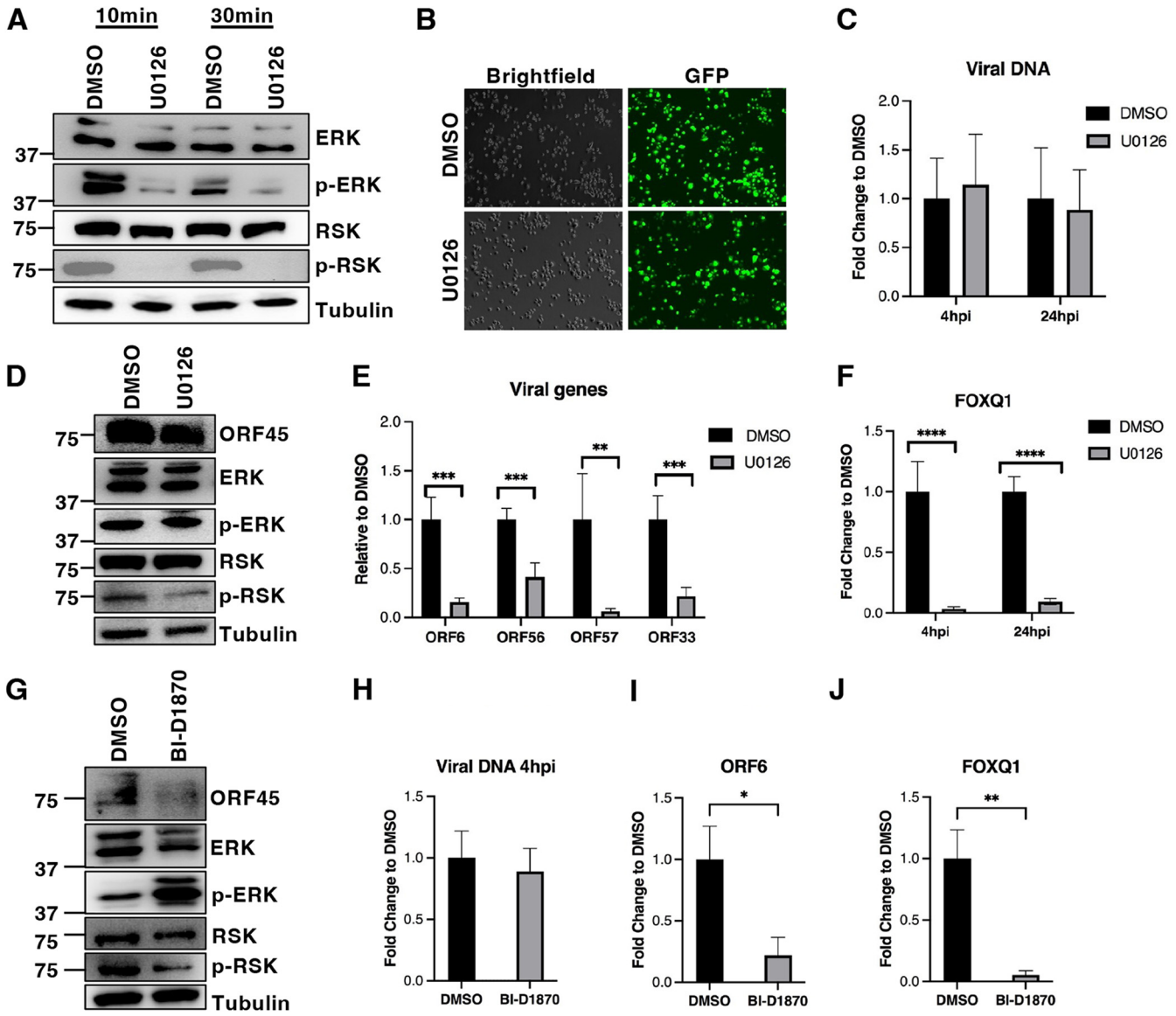

FIG 10 FOXQ1 is not induced during KSHV infection if the ERK/RSK cascade is inhibited. (A) Uninfected TIGK cells were treated with 10 μM MEK inhibitor U0126 or an equivalent volume of DMSO vehicle control for 10 min and 30 min. The effect on ERK and RSK activation was analyzed by immunoblotting. (B to F) TIGK cells were infected with KSHV in the presence of either 10 μM U0126 or the DMSO control and collected at 4 and 24 hpi as indicated. (B) Representative fluorescence image of KSHV-infected TIGK cells at 24 hpi; (C) qPCR analysis of intracellular viral DNA copy in DMSO control- or U0126-treated cells at 4 and 24 hpi; (D) immunoblot analysis of ORF45 and ERK/RSK markers at 4 hpi; (E) RT-qPCR analysis of representative viral genes at 24 hpi; (F) RT-qPCR analysis of FOXQ1 levels in DMSO control- versus U0126-treated cells at 4 and 24 hpi. (G to J) TIGK cells were infected with KSHV in the presence of either 10 μM BI-D1870 or the DMSO control and collected at 4 hpi. (G) Immunoblot analysis of ORF45 and ERK/RSK markers at 4 hpi; (H) qPCR analysis of intracellular viral DNA copy in DMSO-treated or BI-D1870-treated cells at 4 hpi; (I) RT-qPCR analysis of lytic viral ORF6 gene at 4 hpi; (J) RT-qPCR analysis of FOXQ1 levels in DMSO control- versus BI-D1870-treated cells at 4 hpi. *, $P < 0.05$; **, $P < 0.01$; ***, $P < 0.001$; ****, $P < 0.0001$.

(Fig. 9F). These results suggest that FOXQ1 activation is downstream of the ORF45-mediated sustained RSK activations in oral epithelial cells.

Previous studies have shown that treatment with a small molecule inhibitor of MEK1/2 (U0126) resulted in decreased viral and host gene expression during KSHV infection of human foreskin fibroblast cells and during lytic reactivation of latently infected primary effusion lymphoma cells (30, 63, 64). To evaluate the effect of U0126 on downstream ERK/RSK signaling, we treated uninfected TIGK cells for 10 min and 30 min with U0126 and observed reduced p-ERK/p-RSK levels (Fig. 10A). Next, we tested whether U0126 treatment during KSHV infection affects lytic gene expression and FOXQ1 activation in oral epithelial cells. U0126 treatment did not lead to differences in the cellular morphology or in the number of KSHV-infected cells as visualized by GFP

(Fig. 10B) or viral DNA level (Fig. 10C). While a reduced level of p-RSK was observed in U0126-treated KSHV-infected TIGK cells at 4 hpi, p-ERK levels were unaffected by U0126 treatment (Fig. 10D), which could be due to potential engagement of feedback loops that masked the effects of longer U0126 treatments (reviewed in reference 65). It has also been shown that U0126 is less efficient at inhibiting p-ERK activation at 5 h postreactivation than p-RSK, possibly due to the higher overall cellular levels of ERK (32). In line with previous studies in other cell types (30, 63, 64), we observed a reduction of viral gene expression following U0126 treatment (Fig. 10E), indicating that the ERK cascade drives lytic gene expression in infected TIGK cells. Notably, U0126 treatment only slightly reduced ORF45 protein levels at 4 hpi (Fig. 10D), likely due to abundance of incoming ORF45 tegument protein. Importantly, U0126 treatment significantly reduced FOXQ1 expression in KSHV-infected TIGK cells compared to the dimethyl sulfoxide (DMSO) control at both 4 hpi and 24 hpi (Fig. 10F). To more specifically identify the role of RSK, which is downstream of MEK/ERK, we treated cells with small molecule inhibitor BI-D1870, which is specific for RSK and has been shown previously to inhibit KSHV lytic reactivation (32). BI-D1870 treatment during KSHV infection of TIGK cells lead to a decrease in phosphorylated RSK, but not phosphorylated ERK, as expected due to the specificity of the inhibitor for RSK (Fig. 10G). While BI-D1870 treatment did not lead to a significance difference in viral entry as measured by DNA copy at 4 hpi (Fig. 10H), lytic gene expression was defective following RSK inhibition (Fig. 10I). Finally, KSHV-mediated FOXQ1 induction was significantly reduced by BI-D1870 treatment (Fig. 10J). These findings indicate that ORF45-mediated sustained activation of the ERK/RSK pathway is critical for induction of FOXQ1 in oral epithelial cells.

ORF45 is necessary to engage in the ERK/RSK/FOXQ1 lytic cycle-promoting axis in KSHV-infected oral epithelial cells. Finally, we evaluated whether ORF45 was necessary for FOXQ1 induction during primary KSHV infection of oral epithelial cells. While RTA itself was capable of modest induction of FOXQ1 expression in oral epithelial cells, it was not necessary for FOXQ1 induction in the context of KSHV infection, likely due to its redundancy with incoming tegument proteins, mainly ORF45. To test the contribution of ORF45 to FOXQ1 induction, we created a series of KSHV BAC16 clones: (i) a virus encoding a 3×FLAG-tagged ORF45 (3×F-ORF45 KSHV), (ii) an ORF45/RTA double knockout KSHV (3×F-ORF45/RTA dKO) in which stop codons were inserted both in the ORF45 and RTA genes of the 3×F-ORF45 KSHV bacmid, and (iii) a 3×FLAG-tagged ORF45 knockout (3×F-ORF45KO) KSHV in which the additional stop codon in the RTA gene in the 3×F-ORF45/RTA dKO KSHV bacmid was removed (Fig. 11A). First, we infected TIGK cells with 3×F-ORF45 KSHV or 3×F-ORF45/RTA dKO KSHV, which resulted in comparable infection as shown by GFP^+ cells at 24 hpi (Fig. 11B) and by viral copy quantification at 2 hpi and 24 hpi (Fig. 11C). The titer used for this set of mutant viruses was also comparable to the titer used for wild-type virus in previous experiments. As expected, the dKO virus was not only deficient in ERK and RSK activation (Fig. 11D) but also deficient in lytic gene expression at both the mRNA and protein levels (Fig. 11D and E). Strikingly, while FOXQ1 was still induced following infection with 3×F-RTAKO KSHV (Fig. 7D), induction was severely abrogated in dKO-infected TIGK cells (Fig. 11F), highlighting the essential function of ORF45 during infection of oral epithelial cells. To further demonstrate the essential role of ORF45, we infected TIGK cells with equal titers of either 3×F-ORF45 KSHV, 3×F-ORF45/RTA dKO KSHV, and 3×F-ORF45KO KSHV (Fig. 11G). Of note, the titers of viruses used for this experiment were ~10-fold lower than the titer used in previous experiments, due to challenges in creating a high titer of the 3×F-ORF45KO KSHV. We found that 3×F-ORF45KO KSHV was as deficient in lytic viral gene expression as the dKO virus (Fig. 11H) and also failed to induce FOXQ1 (Fig. 11I). In conclusion, these results demonstrate that ORF45 and its ERK/RSK-sustaining activity is an essential trigger for the increased expression of the lytic cycle-promoting FOXQ1 in oral epithelial cells during KSHV infection (Fig. 12).

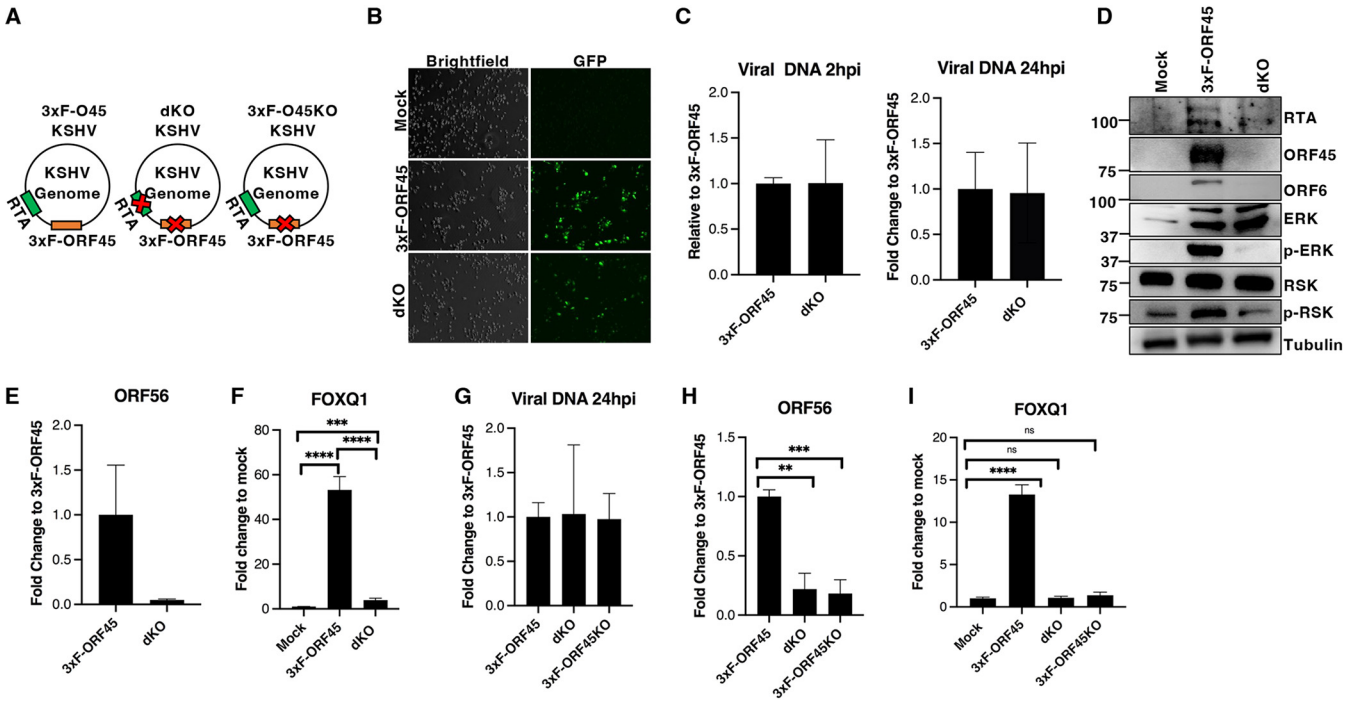

FIG 11 ORF45 is necessary to engage the ERK/RSK/FOXQ1 axis in oral epithelial cells (A) Schematic detailing the N-terminally triple FLAG-tagged ORF45 (3×F-ORF45), 3×F-ORF45/RTA double knockout (dKO), and 3×F-ORF45KO single knockout KSHV bacmids with stop codons in the ORF45 or RTA genes as indicated. (B to F) TIGK cells were infected with equal titers of 3×F-ORF45 KSHV or 3×F-ORF/RTA dKO KSHV and collected at 24 hpi. (B) Representative fluorescence images of KSHV-infected TIGK cells at 24 hpi; (C) qPCR analysis of intracellular viral DNA copy at 2 hpi and 24 hpi; (D) immunoblot of viral genes and ERK/RSK markers at 24 hpi; (E and F) RT-qPCR analysis of viral gene ORF56 expression (E) and RT-qPCR analysis of FOXQ1 levels (F) at 24 hpi. (G to I) TIGK cells were infected with equal titers of 3×F-ORF45 KSHV, 3×F-ORF45/RTA dKO KSHV, or 3×F-ORF45KO KSHV. (G) qPCR analysis of intracellular viral DNA levels at 24 hpi; (H) RT-qPCR analysis of viral gene ORF56 expression; (I) RT-qPCR analysis of FOXQ1 levels at 24 hpi. **, $P < 0.01$; ***, $P < 0.001$; ****, $P < 0.0001$; ns, not significant.

DISCUSSION

Epidemiologic studies indicate the oral route as a primary mode of KSHV transmission, and several groups have demonstrated high rates of viral shedding in saliva in infected individuals (10, 13). The clinical relevance of the oral cavity in KSHV infection prompted us to characterize how KSHV infection progresses in oral epithelial cells. We found that KSHV infection rapidly induced the expression of the host transcription factor FOXQ1 both in primary oral epithelial cells as well as in telomerase-immortalized gingival keratinocytes and that the increase in FOXQ1 expression was accompanied by an accumulation of activating H3K27ac histone marks in the FOXQ1 regulatory region. We also provided evidence that rapid accumulation of FOXQ1 is needed for sustained KSHV lytic protein and viral DNA accumulation up to 4 days following primary infection in oral epithelial cells. Finally, we showed that FOXQ1 induction requires the ORF45-mediated sustained activation of the ERK/RSK signaling pathway, revealing a novel positive feedback loop during KSHV infection in which a viral factor manipulates a host signaling pathway not only to drive lytic gene expression but also to drive rapid host reprogramming to sustain the KSHV lytic cycle.

We identified FOXQ1 as the top induced human gene in primary oral epithelial cells upon KSHV infection at 8 hpi. Interestingly, FOXF2, which is adjacent to FOXQ1 in the human genome, was also among the most induced host genes, which could be due to shared regulatory regions. The FOXQ1 and FOXF2 genes encode members of the Forkhead transcription factor family, which share a conserved winged-helix DNA-binding domain (called the Forkhead domain) and play a role in cellular differentiation, aging, development and disease (66). Several Forkhead factors have been studied in the context of viral infections (51–54), but their function is still largely uncharacterized in the KSHV life cycle. In the context of KSHV, the Forkhead factor FOXO1 has been shown to be critical for maintenance of KSHV latency by regulating the cellular redox

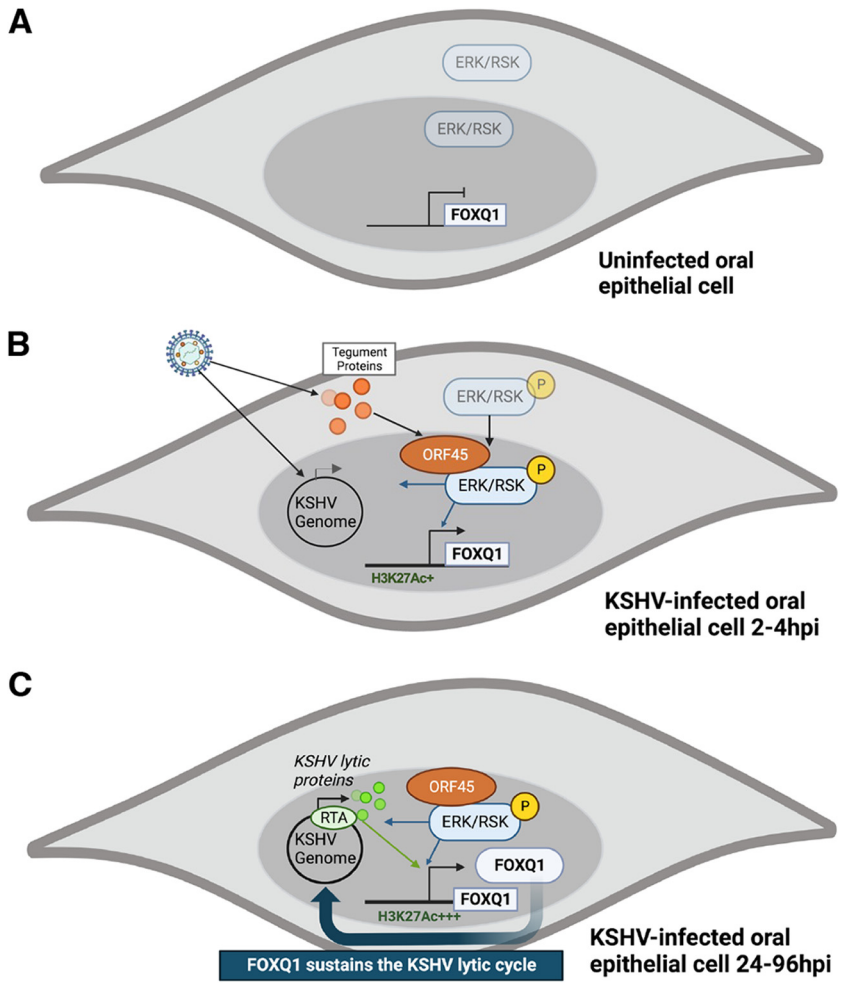

FIG 12 Working model (A) In uninfected oral epithelial cells, ERK/RSK pathway activity is at the basal level, while FOXQ1 gene expression is very low and its promoter lacks substantial levels of activating H3K27ac marks. (B) In the first hours of KSHV infection, the viral genome and virion-associated tegument proteins, including ORF45, are deposited. ORF45 binding to ERK/RSK sustains ERK/RSK phosphorylation levels, driving activation of KSHV lytic gene expression and high FOXQ1 expression in parallel. There is increased H3K27ac mark in the direct vicinity of the transcription start site of the FOXQ1 gene in KSHV-infected cells at 4 hpi. (C) At the end of the first day of infection, a high level of H3K27ac mark accumulation is detected across the entire FOXQ1 promoter region. Increased FOXQ1 protein accumulation is observed in infected cells, and subsequently FOXQ1 contributes to sustaining the KSHV lytic cycle up to 4 days postinfection.

balance (53). Here, we demonstrated that FOXQ1 is induced by KSHV infection and subsequently promotes the KSHV lytic cycle in oral epithelial cells, as siRNA-mediated depletion of FOXQ1 in TIGK cells shortly after KSHV infection resulted in reduced viral copy number and lytic protein levels, both of which were observed up to 4 days following primary infection. Thus, our findings uncover a novel role for FOXQ1 in promoting KSHV lytic infection in oral epithelial cells. This FOXQ1 function is in direct contrast to the lytic cycle-suppressing function of FOXO1 (53) and could be related to the known functional diversity of Forkhead factors. While FOXQ1 has not been studied in the context of gammaherpesvirus infections, it has been associated with various diseases. FOXQ1 is most studied in the context of cancer, and it regulates genes associated with delayed cellular senescence, antiapoptotic activity, and the epithelial-mesenchymal transition (67–69). Future studies are warranted to identify the genome-wide targets of FOXQ1 in oral epithelial cells and to reveal the mechanism by which FOXQ1 promotes the KSHV lytic cycle.

In line with the known role of FOXQ1 in regulating cellular identity, a previous

bioinformatics study also listed FOXQ1 and epidermal differentiation complex (EDC) genes among the genes that are induced during epithelial differentiation-promoting conditions in the skin (50). The epidermal differentiation complex (EDC) is a set of over 50 genes involved in the terminal differentiation of keratinocytes (70). Our transcriptome analysis revealed that only a specific subset of EDC genes (e.g., the LCE3D and LCE3E genes) were rapidly induced during primary KSHV infection of oral epithelial cells. In accordance, we also found enrichment of keratinization and skin differentiation as enriched biological processes among the most induced host genes during KSHV infection. While the functional link between FOXQ1 and the EDC proteins in KSHV infections remains to be investigated, it is known that KSHV infection is enhanced by epithelial differentiation, with augmented lytic gene expression in more terminally differentiated layers of the epithelium (15–17). A recent comprehensive elegant single-cell RNA-seq study with an oral epithelial organoid culture model further highlighted that KSHV infection dysregulates epithelial differentiation and uniquely alters cellular pathways at each epithelial layer, which in turn can support viral lytic replication (16). In this regard, treatment of oral keratinocytes with KSHV-derived virus-like vesicles (VLVs) that lack viral DNA in the virion has also been shown to induce a largely similar set of EDC genes and differentiation-promoting signaling events (43), which aligns with our finding regarding the involvement of tegument proteins such as ORF45. We propose that KSHV infection brings in tegument proteins such as ORF45 which can promote rapid alteration of oral epithelial cells to create a sustained lytic infection-promoting cellular environment. The potential role of Forkhead factors such as FOXQ1 in KSHV infection-induced host alterations remains to be determined. Future studies are warranted to dissect the role of cell-type-specific interplays between incoming viral factors and their host targets in their unique chromatin environments.

While the basal expression of FOXQ1 is very low in uninfected oral epithelial cells, KSHV infection leads to its robust induction within hours of infection. The rapid induction of FOXQ1 expression suggests that the FOXQ1 promoter has a chromatin structure that is poised for rapid activation. In accordance with this, we were able to demonstrate that the FOXQ1 regulatory region carries the H3K4me3 mark, which is present on promoters of either poised or active genes (71). While the H3K4me3 mark was present on the FOXQ1 promoter under both uninfected and infected conditions, the FOXQ1 promoter is largely devoid of the activating H3K27ac mark in uninfected cells. While KSHV infection did not result in widespread alteration of H3K4me3 levels on the FOXQ1 promoter consistently in both HGEP and TIGK cells, it triggered a rapid accumulation of H3K27ac on the FOXQ1 promoter, which began as early as 4 hpi, uncovering a novel KSHV-driven epigenetic reprogramming event that can contribute to the induction of FOXQ1 gene expression.

To identify KSHV factors driving FOXQ1 expression in oral epithelial cells, we evaluated 18 KSHV factors and found that immediate early proteins ORF45 and RTA were capable of upregulating FOXQ1 in HGEP and TIGK cells. ORF45 is both an immediate early protein and part of the viral tegument (39, 72). ORF45 is critical for the production of infectious virions, as ORF45-null KSHV is defective in lytic viral gene expression and virus production (61). The RTA gene is an immediate early gene and is necessary for the KSHV lytic cycle (24, 26, 27). Importantly, although FOXQ1 expression in KSHV-infected oral epithelial cells was tightly tied to viral titer, the RTAKO virus, which was deficient in lytic gene expression, was still able to induce FOXQ1. Our data suggest that FOXQ1 expression could be triggered during RTAKO KSHV infection by incoming virion proteins, such as the tegument protein ORF45. To test this hypothesis and to distinguish the role of RTA and the tegument protein ORF45, we generated ORF45 and RTA double knockout as well as single ORF45 knockout KSHV mutants. We found that RTAKO, RTA/ORF45 dKO, and ORF45KO mutants were all deficient in lytic viral gene expression, yet only the RTA/ORF45 dKO and the ORF45KO mutants were deficient in FOXQ1 induction, indicating ORF45 as the primary inducer of FOXQ1 in oral epithelial cells during KSHV infection. We hypothesize that while RTA by itself can modestly

increase expression of FOXQ1, abundant tegument proteins such as ORF45 might mask any contribution of RTA to FOXQ1 induction during primary infection with KSHV.

ORF45 has several functions during primary infection, including blunting the host interferon response, activating the cellular inflammasome, and modulating host signaling pathways to promote the viral life cycle (32, 38, 73, 74). ORF45 has a nuclear localization signal and nuclear export signal, providing an ability to shuttle between the nucleus and cytoplasm (75), which can be critical for its functionality. In 293T cells, ORF45 has been shown to localize to the cytoplasm, which allows for its IRF7 inhibitory function (38), and is also primarily localized in the cytoplasm of reactivated B-cell lymphoma cells (32). In contrast, we demonstrated that ORF45 has a predominantly nuclear localization in oral epithelial cells at 4 hpi. Since nuclear translocation of ERK/RSK occurs during MAPK activation (76), the predominance of ORF45 and RSK in the nucleus of oral epithelial cells may allow enhanced interactions with nuclear host transcriptional machinery to induce host gene expression. Manipulation of ERK signaling is a common strategy used by DNA viruses to promote cell differentiation, proliferation, and survival (31). While it is known that ORF45-mediated activation of the RSK pathway is essential for infectious virus production (32, 62), here we demonstrated that activation of the ORF45/ERK/RSK axis is also critical for the induction of expression of the lytic cycle-promoting FOXQ1 host gene during KSHV infection of oral epithelial cells. Specifically, we found that mutation of the ORF45 ERK/RSK-interaction domain or inhibition of the MEK/ERK/RSK pathway abrogated FOXQ1 induction. We envision that ORF45-driven sustained activation of ERK/RSK signaling in oral epithelial cells might lead to globally altered cellular gene expression to create a permissive cellular environment that promotes accumulation of lytic viral factors and viral replication. In fact, dynamic ERK signaling is known to be tightly linked to cellular differentiation and proliferation in response to environmental cues (77, 78), and EDC gene expression is also tied to ERK activation (79, 80). It remains to be tested if ORF45 has similar key roles in other cell types as well, as neither KSHV infection nor ORF45 itself was able to induce FOXQ1 expression in the other tested cell types. We envision that the chromatin of the FOXQ1 promoter might be poised for rapid ORF45-triggered induction only in oral epithelial cells but inaccessible in other cell types. Thus, we predict that ORF45 would engage these cellular pathways to fulfill its host gene regulatory function in a highly cell-type-specific manner as guided by the different cellular chromatin environments. Thus, unbiased identification of ORF45 host targets could reveal novel ORF45 and ORF45/ERK/RSK pathway-driven reprogramming events that uniquely support lytic viral infections in the oral epithelium and beyond. Identification and characterization of key ORF45 targets could direct future therapeutic interventions to reduce virus transmission.

MATERIALS AND METHODS

Cell culture, viruses, *de novo* infections. Human gingival epithelial (HGEP) cells (Zen-Bio) were maintained in CnT Prime epithelial culture medium (Zen-Bio) according to the manufacturer's instructions. Telomerase-immortalized gingival keratinocyte (TIGK) cells (ATCC) were maintained in dermal basal cell medium with keratinocyte growth supplement (ATCC). Penicillin-streptomycin (P/S) was only added to HGEP and TIGK culture medium for the final experimental treatments but not during routine culture of oral epithelial cells. HEK293T cells (ATCC) were maintained in Dulbecco's modified Eagle medium (DMEM) containing 10% fetal bovine serum (FBS) and P/S, and 293T cells carrying the KSHV BAC16 clone (293TBAC16) were grown under the same conditions as 293T cells, with the addition of 200 μg/mL hygromycin. iSLK cells were obtained from Jae U Jung, and the origin and generation of iSLK cells were described previously (81). iSLKBAC16 cells were cultured in DMEM with 10% FBS and P/S with 1 mg/mL hygromycin. The procedure for culturing BAC16-3×FLAG-RTA and BAC16-3×FLAG-RTA-KO KSHV was published and described previously (59). The construction of recombinant KSHV BAC16 viruses, establishment of iSLK-BAC16 new recombinant cell lines was done as previously described (42). Bacterial artificial chromosome (BAC)-based recombination was used to generate the 3×FLAG-tagged ORF45, 3×FLAG-tagged ORF45KO/RTAKO, and 3×FLAG-tagged ORF45KO KSHV genomes in *Escherichia coli* strain GS1783. Briefly, we created a KSHV BAC16 clone by epitope tagging the 5′ end of the ORF45 gene with three copies of FLAG epitope tag. The 3×FLAG-tagged ORF45KO/RTAKO double knockout KSHV BAC16 bacmid, which lacks both ORF45 and RTA protein expression, was created by introducing a STOP codon both in the FLAG-tagged ORF45 and RTA gene open reading frames. The RTA knockout was created as previously published (82). The ORF45 knockout was generated by inserting a T nucleotide after nucleotide 26 in the ORF45 open reading frame, resulting in a frameshift and a stop codon. Finally,

TABLE 1 List of primers used in this study

	Primer sequence (5′→3′)	
Gene primer	Forward	Reverse
FOXQ1	CCATAGTCCACCCAACACTTG	TCTACCCTGGTCTTCCGAGAT
18S	TTCGAACGTCTGCCCTATCAA	GATGTGGTAGCCGTTTCTCAGG
Actin	CCACAGCCAGAGGTCCTCAG	AGGAGCTCTTGGAGGGCATG
Intergenic	CAGGATCTCCGAGAATCAGC	GAGTTGGGAGAGCTGTCAGG
−2012	CAGCCCACAGGATAGACATAA	GATCCTCTCCTTACCCTGATTT
−1279	CGAGATTGTCCGACACTGGT	TCACGGCCATTTCTTTCCAATA
−562	GACAGGGGTTTGCTTTCGTAA	GCGTATGTGCTTCTGTAGTAGTG
+98	GGGTGCTCAAGGCTGAAGGC	CGGATGATGTGCGTGCCACC
+214	CCTCCTGGGCTCTTTAACGA	GGGCTTAGAAGGCTTTCCTG
ORF11	GGCACCCATACAGCTTCTACGA	CGTTTACTACTGCACACTGCA
HS1	TTCCTATTTGCCAAGGCAGT	CTCTTCAGCCATCCCAAGAC

the 3×FLAG-tagged ORF45KO KSHV bacmid was created from the 3×FLAG-ORF45KO/RTAKO KSHV BAC16 bacmid by eliminating the STOP codon from the RTA coding region, restoring the intact RTA coding frame. Bacmid DNA was transfected into iSLK cells which were selected and induced for virus production as previously detailed (83). Briefly, iSLK cells containing the BAC16 mutant bacmids were selected with 1 mg/mL hygromycin for several weeks to allow for stable cell line expansion, and all were confirmed to homogenously express green fluorescent protein (GFP) due to the BAC16-encoded constitutively expressed GFP gene marker. KSHV stock was produced by treating iSLKBAC16 with 1 μg/mL doxycycline and 1 mM sodium butyrate (NaB) for 5 days. Virus stocks were rigorously titrated to the corresponding reference control KSHV as described previously (84). For infections, medium for mock- and KSHV-infected cells was changed at 2 hpi and cells were harvested at the indicated time points. 293TBAC16 cells were reactivated using 3 mM NaB. All experiments were performed with a minimum of three biological replicates, and two independent experiments and representative data are shown.

Transfection. For expression of FLAG-tagged FOXQ1, pCMV6-FOXQ1-MYC-FLAG mammalian expression plasmid and pCMV6 control plasmids (both from Origene) were transfected into 293T cells. TIGK cells were infected with KSHV for 2 h and then transfected with siRNAs targeting either FOXQ1 (independent siRNAs against FOXQ1 referred to as siFOXQ1 1 [Dharmacon] or siFOXQ1 2 [Santa Cruz]) or nontargeting negative-control siRNA (siGENOME Dharmacon D-001210-02, targeting firefly luciferase). siRNA transfections were performed with Lipofectamine RNAiMAX reagent (Invitrogen) following the manufacturer's instructions. Transfection reagent was removed after 4 h. Knockdown efficiency of FOXQ1 was assessed using reverse transcription-quantitative PCR (RT-qPCR). For ORF45 expression, TIGK cells were transfected with pCDH-CMV-ORF45 plasmid or the GFP control using Lipofectamine 3000 transfection reagent (Invitrogen). Lipofectamine reagent was removed after 4 h, and fresh medium with penicillin-streptomycin was added. Cells were collected at 30 h post transfection.

Lentiviruses. Lentivirus generation was performed with pCDH-CMV-MCS-EF1puro lentiviral vectors encoding ORF45, the ORF45-F66A mutant, the 3×FLAG-tagged RTA, the indicated viral ORFs, or the GFP control. The ORF45-F66A mutation was previously described and extensively characterized by the laboratory of Fanxiu Zhu (62). Lentiviruses were produced, concentrated, and transduced as previously described (85). Briefly, TIGK or HGEP cells were transduced with lentiviruses in the presence of 8 μg/mL Polybrene and incubated for 6 h before lentiviral medium was exchanged for fresh medium. Cells were harvested 2 days after lentivirus transduction, unless otherwise indicated.

Chemicals and antibodies. The following antibodies were used for immunoblotting and/or immunofluorescence imaging: anti-FLAG (Sigma; F1804), anti-tubulin (Sigma; T5326), normal mouse IgG (catalog no. sc-2025; Santa Cruz), normal rabbit IgG, anti-RTA (from Yoshihiro Izumiya, University of California Davis), anti-ORF6 (from Gary S. Hayward, Johns Hopkins University), anti-ORF45 (catalog no. sc-53883; Santa Cruz), anti-K8.1 (catalog no. sc-65446; Santa Cruz), anti-K2 (catalog no. 251352; Abbiotec) anti-RSK1 (catalog no. 8408S; Cell Signaling), anti-phospho-p90 RSK (Thr359/Ser363) (catalog no. 9344s; Cell Signaling), anti-ERK1/2 (catalog no. 9102, Cell Signaling), anti-phospho-ERK1/2 (Thr202/Tyr204) (catalog no. 9101; Cell Signaling), and anti-FOXQ1 (catalog no. sc-166265; Santa Cruz). For immunoblotting, antibodies were diluted in phosphate-buffered saline-Tween 20 (PBST). Doxycycline (Dox), sodium butyrate (NaB), and phosphonoacetic acid (PAA) were purchased from Sigma. PAA was used at 100 μM to inhibit KSHV replication. The U0126 inhibitor (Sigma) and BI-D1870 inhibitor (Santa Cruz) were used at 10 μM to inhibit ERK and RSK signaling, respectively.

Total RNA purification and RT-qPCR. RNA purification and quantification of gene expression by RT-qPCR were performed as described previously (85). Briefly, equal amounts of total RNA (between 300 ng and 1 μg) were used for cDNA synthesis, and 5-fold-diluted cDNA was analyzed by quantitative PCR (qPCR) to measure the expression of host and viral genes. The qPCR was performed in CFX96 real-time PCR machine using SYBR green (Bio-Rad). Gene expression changes were calculated using the threshold cycle ($\Delta\Delta C_T$) method, in which target gene expression was determined relative to the level of host 18S rRNA and calculated relative to control conditions. For significance testing, a two-tailed Student's *t* test was performed. Primers specific for KSHV were previously published (85). The DNA sequences of oligonucleotides used for qPCR for host genes are listed in Table 1.

Total DNA purification and measuring relative viral copy number. KSHV-infected cells were lysed in radioimmunoprecipitation assay (RIPA) buffer followed by sonication. Total DNA was purified by phenol-chloroform extraction, and 10 ng of total DNA was analyzed by qPCR. The viral DNA was measured by qPCR using primers for ORF11, and the amount of viral DNA was normalized by the cellular DNA input, which was measured by qPCR primers specific for the DNase I hypersensitivity site of the globin gene (HS1) genomic region. The change in viral DNA load between different treatment conditions was calculated using the $\Delta\Delta C_T$ method, where control samples were used as reference points. The DNA sequences of oligonucleotides used for qPCR are listed in Table 1.

RNA-seq analysis. Total RNA was prepared from three replicates of mock- and KSHV-infected HGEP cells at 8 h postinfection. RNA was prepared with Tri reagent (Sigma), purified with an RNeasy kit (Qiagen), and digested with RNase-free DNase (Qiagen). Eluted RNA was sent to a sequencing core facility, which prepared RNA-seq libraries with the KAPA stranded RNA-seq kit using the standard workflow, consisting of mRNA enrichment, cDNA generation, end repair, A-tailing, unique adaptor ligations to allow for multiplexing of samples, strand selection, and PCR amplification, followed by sequencing on Illumina HiSeq3000 with a base read length of 50 and subsequent demultiplexing with Illumina Bcl2fastq2 v.2.17 program. Derived RNA-seq raw data sets were processed using FLOW software build v.10.0.22.1005 (Partek, Inc., St. Louis, MO). Analysis steps included alignment to the hg38 version human genome build using the STAR aligner, followed by the Partek E/M Quantification to RefSeq Transcripts 101—2002-02-01 human transcript annotation model, followed by generation of normalized gene counts with DESeq2 gene-level quantification. Statistical analyses were performed within the FLOW pipeline, resulting in the list of differentially expressed host genes between KSHV-infected and mock-infected samples. We used at least 2-fold differential expression and a step-up Benjamini-Hochberg false-discovery rate correction (FDR) of <0.05. The supplemental material (Tables S1 and S2) provides all of the processed gene expression values with gene counts of all of the detected human genes with gene symbols, as well as the differentially expressed gene lists and the described Gene Ontology (GO) analysis outcomes. GO analysis was performed with DAVID Bioinformatics Resources NIAID/NIH software using the standard Functional Annotation settings with *Homo sapiens* as the species, official gene symbols, and set to obtain all GO terms specifically with the biological process direct settings. Figure 2C and Figure 2D depict the top six identified GO terms for all the upregulated and downregulated genes (cutoff described above), while Table S2 lists the entire outcome with criteria and associated gene names for each of the respective data sets.

Chromatin immunoprecipitation. For chromatin preparation, HGEP or TIGK cells were harvested and cross-linked 4 h or 24 h following KSHV infection or mock infection, as indicated. Cross-linking and chromatin immunoprecipitation of HGEP and TIGK cells were performed as previously described (85). Immunoprecipitation was carried out with 1 μg of H3K27ac (catalog no. 39155; Active Motif) or H3K4me3 (catalog no. 39159; Active Motif) antibodies overnight at 4°C. The enrichment of histone modifications on specific genomic regions was calculated as a percentage of the immunoprecipitated DNA relative to input DNA. The ChIP-qPCR primer sequences are listed in Table 1.

Immunofluorescence. TIGK cells were infected with either KSHV or mock, or lentiviruses as indicated, and these cells were fixed with 4% paraformaldehyde for 10 min, permeabilized by 0.5% Triton X-100 for 5 min, washed twice with PBST, and then incubated in blocking buffer (5% FBS, 0.2% fish skin gelatin, and PBST) for 30 min. Anti-mouse IgG, anti-rabbit IgG, anti-RSK1, and anti-ORF45 antibodies were used to stain cells overnight at 4°C. Cells were washed three times with the PBST washing buffer and incubated with anti-mouse antibody conjugated to Alexa Fluor 647 and anti-rabbit antibody conjugated to Alexa Fluor 555 (Invitrogen) for 1 h at room temperature. Cells were washed with washing buffer with DAPI (4′,6-diamidino-2-phenylindole) added as a DNA stain and imaged with a Revolve fluorescence microscope (Echo Laboratories).

Data availability. The original raw and processed RNA-seq data set is available in the public NCBI GEO database under GEO accession no. GSE223396.

SUPPLEMENTAL MATERIAL

Supplemental material is available online only.

SUPPLEMENTAL FILE 1, DOCX file, 0.02 MB.

SUPPLEMENTAL FILE 2, XLSX file, 2.6 MB.

SUPPLEMENTAL FILE 3, XLSX file, 0.04 MB.

ACKNOWLEDGMENTS

We thank Jae U. Jung, Gary S. Hayward, and Yoshihiro Izumiya for providing reagents. We thank members of the Papp lab and Toth lab for stimulating discussions. In addition, we thank Seung Jin Jang for help during the lentivirus screen and Katherine Glickman, Thomas H. Nguyen, and Juan D. Alonso for excellent technical support.

This study was in part supported by National Institute of Dental and Craniofacial Research (NIDCR) grants R01DE028331 and R03DE028029 as well as the National Institute of Allergy and Infectious Diseases (NIAID) grant R01A1132554, American Cancer Society Research Scholar grant RSG-18-221-01-MPC, and the UF Research Opportunity Seed Fund. N.A. was supported by NIH/NIDCR training grant T90DE021990 and NIH/NIDCR fellowship

F30DE030666, as well as an American Association for Dental Oral and Craniofacial Research (AADOCR) student research fellowship.

REFERENCES

1. Bomsel M, Alfsen A. 2003. Entry of viruses through the epithelial barrier: pathogenic trickery. Nat Rev Mol Cell Biol 4:57–68. https://doi.org/10.1038/nrm1005.
2. Corstjens PL, Abrams WR, Malamud D. 2016. Saliva and viral infections. Periodontol 2000 70:93–110. https://doi.org/10.1111/prd.12112.
3. Hadinoto V, Shapiro M, Sun CC, Thorley-Lawson DA. 2009. The dynamics of EBV shedding implicate a central role for epithelial cells in amplifying viral output. PLoS Pathog 5:e1000496. https://doi.org/10.1371/journal.ppat.1000496.
4. Sacks SL, Griffiths PD, Corey L, Cohen C, Cunningham A, Dusheiko GM, Self S, Spruance S, Stanberry LR, Wald A, Whitley RJ. 2004. HSV shedding. Antiviral Res 63(Suppl 1):S19–S26. https://doi.org/10.1016/j.antiviral.2004.06.004.
5. Minhas V, Wood C. 2014. Epidemiology and transmission of Kaposi's sarcoma-associated herpesvirus. Viruses 6:4178–4194. https://doi.org/10.3390/v6114178.
6. Chang Y, Cesarman E, Pessin MS, Lee F, Culpepper J, Knowles DM, Moore PS. 1994. Identification of herpesvirus-like DNA sequences in AIDS-associated Kaposi's sarcoma. Science 266:1865–1869. https://doi.org/10.1126/science.7997879.
7. Cesarman E, Chang Y, Moore PS, Said JW, Knowles DM. 1995. Kaposi's sarcoma-associated herpesvirus-like DNA sequences in AIDS-related body-cavity-based lymphomas. N Engl J Med 332:1186–1191. https://doi.org/10.1056/NEJM199505043321802.
8. Soulier J, Grollet L, Oksenhendler E, Cacoub P, Cazals-Hatem D, Babinet P, d'Agay MF, Clauvel JP, Raphael M, Degos L. 1995. Kaposi's sarcoma-associated herpesvirus-like DNA sequences in multicentric Castleman's disease. Blood 86:1276–1280. https://doi.org/10.1182/blood.V86.4.1276.bloodjournal8641276.
9. Uldrick TS, Wang V, O'Mahony D, Aleman K, Wyvill KM, Marshall V, Steinberg SM, Pittaluga S, Maric I, Whitby D, Tosato G, Little RF, Yarchoan R. 2010. An interleukin-6-related systemic inflammatory syndrome in patients co-infected with Kaposi sarcoma-associated herpesvirus and HIV but without multicentric Castleman disease. Clin Infect Dis 51:350–358. https://doi.org/10.1086/654798.
10. Casper C, Krantz E, Selke S, Kuntz SR, Wang J, Huang ML, Pauk JS, Corey L, Wald A. 2007. Frequent and asymptomatic oropharyngeal shedding of human herpesvirus 8 among immunocompetent men. J Infect Dis 195:30–36. https://doi.org/10.1086/509621.
11. Webster-Cyriaque J, Duus K, Cooper C, Duncan M. 2006. Oral EBV and KSHV infection in HIV. Adv Dent Res 19:91–95. https://doi.org/10.1177/154407370601900118.
12. Duus KM, Lentchitsky V, Wagenaar T, Grose C, Webster-Cyriaque J. 2004. Wild-type Kaposi's sarcoma-associated herpesvirus isolated from the oropharynx of immune-competent individuals has tropism for cultured oral epithelial cells. J Virol 78:4074–4084. https://doi.org/10.1128/jvi.78.8.4074-4084.2004.
13. Pauk J, Huang ML, Brodie SJ, Wald A, Koelle DM, Schacker T, Celum C, Selke S, Corey L. 2000. Mucosal shedding of human herpesvirus 8 in men. N Engl J Med 343:1369–1377. https://doi.org/10.1056/NEJM200011093431904.
14. Vieira J, Huang ML, Koelle DM, Corey L. 1997. Transmissible Kaposi's sarcoma-associated herpesvirus (human herpesvirus 8) in saliva of men with a history of Kaposi's sarcoma. J Virol 71:7083–7087. https://doi.org/10.1128/JVI.71.9.7083-7087.1997.
15. Johnson AS, Maronian N, Vieira J. 2005. Activation of Kaposi's sarcoma-associated herpesvirus lytic gene expression during epithelial differentiation. J Virol 79:13769–13777. https://doi.org/10.1128/JVI.79.21.13769-13777.2005.
16. Jung KL, Choi UY, Park A, Foo SS, Kim S, Lee SA, Jung JU. 2022. Single-cell analysis of Kaposi's sarcoma-associated herpesvirus infection in three-dimensional air-liquid interface culture model. PLoS Pathog 18:e1010775. https://doi.org/10.1371/journal.ppat.1010775.
17. Seifi A, Weaver EM, Whipple ME, Ikoma M, Farrenberg J, Huang ML, Vieira J. 2011. The lytic activation of KSHV during keratinocyte differentiation is dependent upon a suprabasal position, the loss of integrin engagement, and calcium, but not the interaction of cadherins. Virology 410:17–29. https://doi.org/10.1016/j.virol.2010.10.023.
18. Hassman LM, Ellison TJ, Kedes DH. 2011. KSHV infects a subset of human tonsillar B cells, driving proliferation and plasmablast differentiation. J Clin Invest 121:752–768. https://doi.org/10.1172/JCI44185.
19. Myoung J, Ganem D. 2011. Active lytic infection of human primary tonsillar B cells by KSHV and its noncytolytic control by activated $CD4^+$ T cells. J Clin Invest 121:1130–1140. https://doi.org/10.1172/JCI43755.
20. Aalam F, Nabiee R, Castano JR, Totonchy J. 2020. Analysis of KSHV B lymphocyte lineage tropism in human tonsil reveals efficient infection of $CD138^+$ plasma cells. PLoS Pathog 16:e1008968. https://doi.org/10.1371/journal.ppat.1008968.
21. Atyeo N, Rodriguez MD, Papp B, Toth Z. 2021. Clinical manifestations and epigenetic regulation of oral herpesvirus infections. Viruses 13:681. https://doi.org/10.3390/v13040681.
22. Gunther T, Grundhoff A. 2010. The epigenetic landscape of latent Kaposi sarcoma-associated herpesvirus genomes. PLoS Pathog 6:e1000935. https://doi.org/10.1371/journal.ppat.1000935.
23. Toth Z, Brulois K, Lee HR, Izumiya Y, Tepper C, Kung HJ, Jung JU. 2013. Biphasic euchromatin-to-heterochromatin transition on the KSHV genome following de novo infection. PLoS Pathog 9:e1003813. https://doi.org/10.1371/journal.ppat.1003813.
24. Sun R, Lin SF, Gradoville L, Yuan Y, Zhu FX, Miller G. 1998. A viral gene that activates lytic cycle expression of Kaposi's sarcoma-associated herpesvirus. Proc Natl Acad Sci U S A 95:10866–10871. https://doi.org/10.1073/pnas.95.18.10866.
25. Papp B, Motlagh N, Smindak RJ, Jin Jang S, Sharma A, Alonso JD, Toth Z. 2019. Genome-wide identification of direct RTA targets reveals key host factors for Kaposi's sarcoma-associated herpesvirus lytic reactivation. J Virol 93:01978-18. https://doi.org/10.1128/JVI.01978-18.
26. Lukac DM, Renne R, Kirshner JR, Ganem D. 1998. Reactivation of Kaposi's sarcoma-associated herpesvirus infection from latency by expression of the ORF 50 transactivator, a homolog of the EBV R protein. Virology 252:304–312. https://doi.org/10.1006/viro.1998.9486.
27. Lukac DM, Kirshner JR, Ganem D. 1999. Transcriptional activation by the product of open reading frame 50 of Kaposi's sarcoma-associated herpesvirus is required for lytic viral reactivation in B cells. J Virol 73:9348–9361. https://doi.org/10.1128/JVI.73.11.9348-9361.1999.
28. Bechtel JT, Liang Y, Hvidding J, Ganem D. 2003. Host range of Kaposi's sarcoma-associated herpesvirus in cultured cells. J Virol 77:6474–6481. https://doi.org/10.1128/jvi.77.11.6474-6481.2003.
29. Naranatt PP, Akula SM, Zien CA, Krishnan HH, Chandran B. 2003. Kaposi's sarcoma-associated herpesvirus induces the phosphatidylinositol 3-kinase-PKC-zeta-MEK-ERK signaling pathway in target cells early during infection: implications for infectivity. J Virol 77:1524–1539. https://doi.org/10.1128/jvi.77.2.1524-1539.2003.
30. Sharma-Walia N, Krishnan HH, Naranatt PP, Zeng L, Smith MS, Chandran B. 2005. ERK1/2 and MEK1/2 induced by Kaposi's sarcoma-associated herpesvirus (human herpesvirus 8) early during infection of target cells are essential for expression of viral genes and for establishment of infection. J Virol 79:10308–10329. https://doi.org/10.1128/JVI.79.16.10308-10329.2005.
31. DuShane JK, Maginnis MS. 2019. Human DNA virus exploitation of the MAPK-ERK cascade. Int J Mol Sci 20:3427. https://doi.org/10.3390/ijms20143427.
32. Kuang E, Tang QY, Maul GG, Zhu FX. 2008. Activation of p90 ribosomal S6 kinase by ORF45 of Kaposi's sarcoma-associated herpesvirus and its role in viral lytic replication. J Virol 82:1838–1850. https://doi.org/10.1128/JVI.02119-07.
33. Anjum R, Blenis J. 2008. The RSK family of kinases: emerging roles in cellular signalling. Nat Rev Mol Cell Biol 9:747–758. https://doi.org/10.1038/nrm2509.
34. Kuang E, Wu FY, Zhu FX. 2009. Mechanism of sustained activation of ribosomal S6 kinase (RSK) and ERK by Kaposi sarcoma-associated herpesvirus ORF45 multiprotein complexes retain active phosphorylated ERK and RSK and protect them from dephosphorylation. J Biol Chem 284:13958–13968. https://doi.org/10.1074/jbc.M900025200.
35. Kuang ES, Fu BS, Liang QM, Myoung J, Zhu FX. 2011. Phosphorylation of eukaryotic translation initiation factor 4B (EIF4B) by open reading frame 45/p90 ribosomal S6 kinase (ORF45/RSK) signaling axis facilitates protein translation during Kaposi sarcoma-associated herpesvirus (KSHV) lytic

replication. J Biol Chem 286:41171–41182. https://doi.org/10.1074/jbc.M111.280982.
36. Li XJ, Du SM, Avey D, Li YQ, Zhu FX, Kuang ES. 2015. ORF45-mediated prolonged c-Fos accumulation accelerates viral transcription during the late stage of lytic replication of Kaposi's sarcoma-associated herpesvirus. J Virol 89:6895–6906. https://doi.org/10.1128/JVI.00274-15.
37. Li XJ, Kuang ES. 2015. RSK-c-Fos in KSHV lytic progression. Oncotarget 6:24588–24589. https://doi.org/10.18632/oncotarget.5262.
38. Zhu FX, King SM, Smith EJ, Levy DE, Yuan Y. 2002. A Kaposi's sarcoma-associated herpesviral protein inhibits virus-mediated induction of type I interferon by blocking IRF-7 phosphorylation and nuclear accumulation. Proc Natl Acad Sci U S A 99:5573–5578. https://doi.org/10.1073/pnas.082420599.
39. Zhu FX, Yuan Y. 2003. The ORF45 protein of Kaposi's sarcoma-associated herpesvirus is associated with purified virions. J Virol 77:4221–4230. https://doi.org/10.1128/jvi.77.7.4221-4230.2003.
40. Zhu FX, Chong JM, Wu LJ, Yuan Y. 2005. Virion proteins of Kaposi's sarcoma-associated herpesvirus. J Virol 79:800–811. https://doi.org/10.1128/JVI.79.2.800-811.2005.
41. Atyeo N, Papp B. 2022. The ORF45 protein of Kaposi's sarcoma-associated herpesvirus and its critical role in the viral life cycle. Viruses 14:2010. https://doi.org/10.3390/v14092010.
42. Brulois KF, Chang H, Lee ASY, Ensser A, Wong LY, Toth Z, Lee SH, Lee HR, Myoung J, Ganem D, Oh TK, Kim JF, Gao SJ, Jung JU. 2012. Construction and manipulation of a new Kaposi's sarcoma-associated herpesvirus bacterial artificial chromosome clone. J Virol 86:9708–9720. https://doi.org/10.1128/JVI.01019-12.
43. Gong D, Dai X, Xiao Y, Du Y, Chapa TJ, Johnson JR, Li X, Krogan NJ, Deng H, Wu TT, Sun R. 2017. Virus-like vesicles of Kaposi's sarcoma-associated herpesvirus activate lytic replication by triggering differentiation signaling. J Virol 91:e00362-17. https://doi.org/10.1128/JVI.00362-17.
44. Bagati A, Bianchi-Smiraglia A, Moparthy S, Kolesnikova K, Fink EE, Kolesnikova M, Roll MV, Jowdy P, Wolff DW, Polechetti A, Yun DH, Lipchick BC, Paul LM, Wrazen B, Moparthy K, Mudambi S, Morozevich GE, Georgieva SG, Wang JM, Shafirstein G, Liu S, Kandel ES, Berman AE, Box NF, Paragh G, Nikiforov MA. 2018. FOXQ1 controls the induced differentiation of melanocytic cells. Cell Death Differ 25:1040–1049. https://doi.org/10.1038/s41418-018-0066-y.
45. Xiang LS, Zheng JM, Zhang MD, Ai TT, Cai B. 2020. FOXQ1 promotes the osteogenic differentiation of bone mesenchymal stem cells via Wnt/beta-catenin signaling by binding with ANXA2. Stem Cell Res Ther 11:403. https://doi.org/10.1186/s13287-020-01928-9.
46. Potter CS, Peterson RL, Barth JL, Pruett ND, Jacobs DF, Kern MJ, Argraves WS, Sundberg JP, Awgulewitsch A. 2006. Evidence that the satin hair mutant gene Foxq1 is among multiple and functionally diverse regulatory targets for Hoxc13 during hair follicle differentiation. J Biol Chem 281:29245–29255. https://doi.org/10.1074/jbc.M603646200.
47. Reyahi A, Nik AM, Ghiami M, Gritli-Linde A, Ponten F, Johansson BR, Carlsson P. 2015. Foxf2 is required for brain pericyte differentiation and development and maintenance of the blood-brain barrier. Dev Cell 34:19–32. https://doi.org/10.1016/j.devcel.2015.05.008.
48. Aitola M, Carlsson P, Mahlapuu M, Enerbäck S, Pelto-Huikko M. 2000. Forkhead transcription factor FoxF2 is expressed in mesodermal tissues involved in epithelio-mesenchymal interactions. Dev Dyn 218:136–149. https://doi.org/10.1002/(SICI)1097-0177(200005)218:1%3C136::AID-DVDY12%3E3.0.CO;2-U.
49. Feuerborn A, Srivastava PK, Küffer S, Grandy WA, Sijmonsma TP, Gretz N, Brors B, Gröne HJ. 2011. The Forkhead factor FoxQ1 influences epithelial differentiation. J Cell Physiol 226:710–719. https://doi.org/10.1002/jcp.22385.
50. Egolf S, Aubert Y, Doepner M, Anderson A, Maldonado-Lopez A, Pacella G, Lee J, Ko EK, Zou J, Lan Y, Simpson CL, Ridky T, Capell BC. 2019. LSD1 inhibition promotes epithelial differentiation through derepression of fate-determining transcription factors. Cell Rep 28:1981–1992.e7. https://doi.org/10.1016/j.celrep.2019.07.058.
51. Ramezani A, Nikravesh H, Faghihloo E. 2019. The roles of FOX proteins in virus-associated cancers. J Cell Physiol 234:3347–3361. https://doi.org/10.1002/jcp.27295.
52. Laura MV, de la Cruz-Herrera CF, Ferreiros A, Baz-Martinez M, Lang V, Vidal A, Munoz-Fontela C, Rodriguez MS, Collado M, Rivas C. 2015. KSHV latent protein LANA2 inhibits sumo2 modification of p53. Cell Cycle 14:277–282. https://doi.org/10.4161/15384101.2014.980657.
53. Gao RY, Li TT, Tan B, da Silva SR, Jung JU, Feng PH, Gao SJ. 2019. FoxO1 suppresses Kaposi's sarcoma-associated herpesvirus lytic replication and controls viral latency. J Virol 93:e01681-18. https://doi.org/10.1128/JVI.01681-18.
54. Okumura N, Ikeda M, Satoh S, Dansako H, Sugiyama M, Mizokami M, Kato N. 2015. Negative regulation of hepatitis B virus replication by forkhead box protein A in human hepatoma cells. FEBS Lett 589:1112–1118. https://doi.org/10.1016/j.febslet.2015.03.022.
55. Wu J-j, Li W, Shao Y, Avey D, Fu B, Gillen J, Hand T, Ma S, Liu X, Miley W, Konrad A, Neipel F, Stürzl M, Whitby D, Li H, Zhu F. 2015. Inhibition of cGAS DNA sensing by a herpesvirus virion protein. Cell Host Microbe 18:333–344. https://doi.org/10.1016/j.chom.2015.07.015.
56. Gregory SM, Davis BK, West JA, Taxman DJ, Matsuzawa S, Reed JC, Ting JPY, Damania B. 2011. Discovery of a viral NLR homolog that inhibits the inflammasome. Science 331:330–334. https://doi.org/10.1126/science.1199478.
57. Kaul R, Purushothaman P, Uppal T, Verma SC. 2019. KSHV lytic proteins K-RTA and K8 bind to cellular and viral chromatin to modulate gene expression. PLoS One 14:e0215394. https://doi.org/10.1371/journal.pone.0215394.
58. Guito J, Lukac DM. 2012. KSHV Rta promoter specification and viral reactivation. Front Microbiol 3:30. https://doi.org/10.3389/fmicb.2012.00030.
59. Lee SC, Toth Z. 2022. PRC1-independent binding and activity of RYBP on the KSHV genome during de novo infection. PLoS Pathog 18:e1010801. https://doi.org/10.1371/journal.ppat.1010801.
60. Vieira J, O'Hearn PM. 2004. Use of the red fluorescent protein as a marker of Kaposi's sarcoma-associated herpesvirus lytic gene expression. Virology 325:225–240. https://doi.org/10.1016/j.virol.2004.03.049.
61. Zhu FX, Li XJ, Zhou FC, Gao SH, Yuan Y. 2006. Functional characterization of Kaposi's sarcoma-associated herpesvirus ORF45 by bacterial artificial chromosome-based mutagenesis. J Virol 80:12187–12196. https://doi.org/10.1128/JVI.01275-06.
62. Fu BS, Kuang E, Li WW, Avey D, Li XJ, Turpin Z, Valdes A, Brulois K, Myoung JJ, Zhu FX. 2015. Activation of p90 ribosomal S6 kinases by ORF45 of Kaposi's sarcoma-associated herpesvirus is critical for optimal production of infectious viruses. J Virol 89:195–207. https://doi.org/10.1128/JVI.01937-14.
63. Xie JP, Ajibade AO, Ye FC, Kuhne K, Gao SJ. 2008. Reactivation of Kaposi's sarcoma-associated herpesvirus from latency requires MEK/ERK, JNK and p38 multiple mitogen-activated protein kinase pathways. Virology 371:139–154. https://doi.org/10.1016/j.virol.2007.09.040.
64. Yu FQ, Harada JN, Brown HJ, Deng HY, Song MJ, Wu TT, Kato-Stankiewicz J, Nelson CG, Vieira J, Tamanoi F, Chanda SK, Sun R. 2007. Systematic identification of cellular signals reactivating Kaposi sarcoma-associated herpesvirus. PLoS Pathog 3:e44. https://doi.org/10.1371/journal.ppat.0030044.
65. Lake D, Correa SAL, Muller J. 2016. Negative feedback regulation of the ERK1/2 MAPK pathway. Cell Mol Life Sci 73:4397–4413. https://doi.org/10.1007/s00018-016-2297-8.
66. Benayoun BA, Caburet S, Veitia RA. 2011. Forkhead transcription factors: key players in health and disease. Trends Genet 27:224–232. https://doi.org/10.1016/j.tig.2011.03.003.
67. Zhang H, Meng F, Liu G, Zhang B, Zhu J, Wu F, Ethier SP, Miller F, Wu G. 2011. Forkhead transcription factor foxq1 promotes epithelial-mesenchymal transition and breast cancer metastasis. Cancer Res 71:1292–1301. https://doi.org/10.1158/0008-5472.CAN-10-2825.
68. Zhang X, Wang L, Wang Y, Shi S, Zhu H, Xiao F, Yang J, Yang A, Hao X. 2016. Inhibition of FOXQ1 induces apoptosis and suppresses proliferation in prostate cancer cells by controlling BCL11A/MDM2 expression. Oncol Rep 36:2349–2356. https://doi.org/10.3892/or.2016.5018.
69. Wang P, Lv C, Zhang T, Liu J, Yang J, Guan F, Hong T. 2017. FOXQ1 regulates senescence-associated inflammation via activation of SIRT1 expression. Cell Death Dis 8:e2946. https://doi.org/10.1038/cddis.2017.340.
70. Kypriotou M, Huber M, Hohl D. 2012. The human epidermal differentiation complex: cornified envelope precursors, S100 proteins and the 'fused genes' family. Exp Dermatol 21:643–649. https://doi.org/10.1111/j.1600-0625.2012.01472.x.
71. Voigt P, Tee WW, Reinberg D. 2013. A double take on bivalent promoters. Genes Dev 27:1318–1338. https://doi.org/10.1101/gad.219626.113.
72. Zhu FX, Cusano T, Yuan Y. 1999. Identification of the immediate-early transcripts of Kaposi's sarcoma-associated herpesvirus. J Virol 73:5556–5567. https://doi.org/10.1128/JVI.73.7.5556-5567.1999.
73. Yang X, Zhou JF, Liu CR, Qu YF, Wang WL, Xiao MZX, Zhu FX, Liu ZS, Liang QM. 2022. KSHV-encoded ORF45 activates human NLRP1 inflammasome. Nat Immunol 23:916–926. https://doi.org/10.1038/s41590-022-01199-x.
74. Zhu FX, Sathish N, Yuan Y. 2010. Antagonism of host antiviral responses by Kaposi's sarcoma-associated herpesvirus tegument protein ORF45. PLoS One 5:e10573. https://doi.org/10.1371/journal.pone.0010573.

75. Li XJ, Zhu FX. 2009. Identification of the nuclear export and adjacent nuclear localization signals for ORF45 of Kaposi's sarcoma-associated herpesvirus. J Virol 83:2531–2539. https://doi.org/10.1128/JVI.02209-08.
76. Chen RH, Sarnecki C, Blenis J. 1992. Nuclear localization and regulation of ERK-encoded and RSK-encoded protein kinases. Mol Cell Biol 12:915–927. https://doi.org/10.1128/mcb.12.3.915-927.1992.
77. Hamilton WB, Brickman JM. 2014. Erk signaling suppresses embryonic stem cell self-renewal to specify endoderm. Cell Rep 9:2056–2070. https://doi.org/10.1016/j.celrep.2014.11.032.
78. Yang SH, Kalkan T, Morrisroe C, Smith A, Sharrocks AD. 2012. A genome-wide RNAi screen reveals MAP kinase phosphatases as key ERK pathway regulators during embryonic stem cell differentiation. PLoS Genet 8: e1003112. https://doi.org/10.1371/journal.pgen.1003112.
79. Wurm S, Zhang JS, Guinea-Viniegra J, Garcia F, Munoz J, Bakiri L, Ezhkova E, Wagner EF. 2015. Terminal epidermal differentiation is regulated by the interaction of Fra-2/AP-1 with Ezh2 and ERK1/2. Genes Dev 29: 144–156. https://doi.org/10.1101/gad.249748.114.
80. Cursons J, Gao J, Hurley DG, Print CG, Dunbar PR, Jacobs MD, Crampin EJ. 2015. Regulation of ERK-MAPK signaling in human epidermis. BMC Syst Biol 9. https://doi.org/10.1186/s12918-015-0187-6.
81. Myoung J, Ganem D. 2011. Generation of a doxycycline-inducible KSHV producer cell line of endothelial origin: maintenance of tight latency with efficient reactivation upon induction. J Virol Methods 174:12–21. https://doi.org/10.1016/j.jviromet.2011.03.012.
82. Toth Z, Brulois KF, Wong LY, Lee HR, Chung B, Jung JU. 2012. Negative elongation factor-mediated suppression of RNA polymerase II elongation of Kaposi's sarcoma-associated herpesvirus lytic gene expression. J Virol 86:9696–9707. https://doi.org/10.1128/JVI.01012-12.
83. Golas G, Jang SJ, Naik NG, Alonso JD, Papp B, Toth Z. 2020. Comparative analysis of the viral interferon regulatory factors of KSHV for their requisite for virus production and inhibition of the type I interferon pathway. Virology 541:160–173. https://doi.org/10.1016/j.virol.2019.12.011.
84. Toth Z, Papp B, Brulois K, Choi YJ, Gao SJ, Jung JU. 2016. LANA-mediated recruitment of host polycomb repressive complexes onto the KSHV genome during de novo infection. PLoS Pathog 12:e1005878. https://doi.org/10.1371/journal.ppat.1005878.
85. Toth Z, Smindak RJ, Papp B. 2017. Inhibition of the lytic cycle of Kaposi's sarcoma-associated herpesvirus by cohesin factors following de novo infection. Virology 512:25–33. https://doi.org/10.1016/j.virol.2017.09.001.